ANSYS FLUENT AIDED VISCOUS FLOW MODELLING OF LID DRIVEN CAVITY FLOW, 2D AND 3D FLOW OVER A CYLINDER

By

CHIEMEZUO EMMANUEL UMEAKA- 40083038

SEYEDJAVAD ZIAEIASL – 40107977

NIMA AZHIR – 40087568

MOHAMMADSALEH KHAYYAT – 40088507

To

DR. ALEJANDRO ALLIEVI

Design Project of MECH 6201 (Fluid Mechanics)

Department of Mechanical, Industrial and Aerospace Engineering

Concordia University

17th June, 2019.

ABSTRACT

Analytical equations such as Burgers, Convection – Diffusion, and unsteady incompressible Naiver-Stokes equations are employed to accurately solve or model different incompressible laminar flow problems in 2D space but, it is impossible to use them to solve incompressible laminar flow problems in 3D space. In solving laminar flow problems in this project, in 3D space or to verify the 2D analytical results, Computational Fluid Dynamics (ANSYS Fluent software) is used to model the problems. With all this in mind, the main aim of this project is to show the interaction between fluid viscosity and a body or cavity. Transient fluent analysis is used for these flow problems because the expected results are in the unsteady flow domain. The various ANSYS results obtained for each of the flow conditions are compared with the analytical results provided by the published paper "**Finite element modified method of characteristics for the Navier–Stokes equations**" by Alejandro Allievi and Rodolfo Bermejo [1].

Keywords: CFD, incompressible laminar flow, unsteady Naiver-Stokes equations.

TABLE OF CONTENTS

1. INTRODUCTION 1

1.1. DESCRIPTION OF THE VISCOUS FLOW PROBLEMS 1

1.1.1. 2D Lid Driven Cavity Flow 1

1.1.2. 2D Flow Around Circular Cylinder For Re =100 1

1.1.3. 3D Flow Around Circular Cylinder For Re =100 2

1.2. LITERATURE REVIEW OF PAST CONTRIBUTIONS 2

1.2.1. Use of Finite Element Modified Method of Characteristics for the Navier–Stokes Equations [1]. 2

1.2.2. Ghia et Al [2], Koseff and Street [3] [4]. 3

1.2.3. The Experimental Determination Effects Of Waves On Vortex Shedding From Cylinders [5] 3

1.2.4. Benque´ et al [6], Douglas and Russell and Pironneau [7]. 3

2. THEORY, FUNDAMENTAL EQUATIONS AND BOUNDARY CONDITIONS USED IN FLOW MODELLING 4

2.1. THEORY 4

2.2. FUNDAMENTAL EQUATIONS 5

2.3. FLOW PROBLEMS BOUNDARY CONDITIONS 7

2.3.1. 2D lid driven cavity flow. 7

 Analysis Assumptions and Parameter Description. 8

2.3.2. 2D flow around a circular cylinder for Re =100. 9

 Analysis Assumptions and Parameter Description. 9

2.3.3. 3D flow around a circular cylinder for Re =100. 10

 Analysis Assumptions and Parameter Description. 10

3. NUMERICAL METHODS AND SOLUTION ALGORITHM USED 11

3.1. NUMERICAL METHOD USED 11

3.1.1. Overall Discretization Method 11

 Temporal Discretization [10] 11

 Implicit Time Integration [10] 12

3.1.2. Discretization of the Momentum Equation [10] 13

3.1.3. Discretization of the Continuity Equation [10] 13

3.2. SOLUTION ALGORITHM USED 14

3.2.1. Pressure Based Solver Algorithms [10] 14

3.1.1.1. Pressure Based Segregated Algorithms. [10] 15

 Step By Step Process Used By Pressure Based Segregated Algorithm To Achieve Convergence. 15

- Flow Chart Representing The Above Steps 16
- Actual Pressure Based Segregated Algorithms 16

4. RESULTS 18

4.1. 2D LID DRIVEN CAVITY FLOW 18

4.1.1. Geometry Modelling 18

4.1.2. Geometry Meshing 19

4.1.3. Computational Conditions 21

4.1.4. Flow and Analysis Conditions 21

4.1.5. ANSYS Modelling Output 22

- Cavity Flow Streamline Visualization 22
- U and V velocity Components Comparison Plots for Re= 3200 and 10000 23
- Conclusion 25

4.2. 2D Flow Around Circular Cylinder For Re =100 25

4.2.1. Geometry Modelling 25

4.2.2. Geometry Meshing 27

4.2.3. Computational Conditions 29

4.2.4. Flow Conditions 29

4.2.5. ANSYS Modelling Output 30

- 2D Flow around a Circular Cylinder @ Re=100 Streamline Visualization 30

4.2.6. Conclusion With Lift and Drag Coefficient plot 31

- Conclusion 34

4.3. 3D Flow Around Circular Cylinder For Re =100 34

4.3.1. Geometry Modelling 34

4.3.2. Geometry Meshing 35

4.3.3. Computational Conditions 35

4.3.4. Flow Conditions 36

4.3.5. ANSYS Modelling Output 36

- 2D Flow around a Circular Cylinder @ Re=100 Streamline Visualization 36

4.3.6. Conclusion With Lift and Drag Coefficient plot 38

- Conclusion 41

5. OVERALL CONCLUSION 42

6. REFERENCES ..... A

LIST OF FIGURES

Figure 1: 2D Lid Driven Cavity Boundary Condition Diagram 7
Figure 2: 2D Flow around a Cylinder Boundary Condition Diagram 9
Figure 3: 3D Flow around a Cylinder Boundary Condition Diagram 10
Figure 4: Flow Chart of Working Pressure Based Segregated Algorithm..... 16
Figure 5: Sketcher 2D Box 18
Figure 6: Converted 2D Plane..... 19
Figure 7: 2D Flow over a Cylinder Final Mesh Outcome 20
Figure 8: Cavity Flow at Re 3200..... 22
Figure 9: Cavity Flow at Re 10000..... 23
Figure 10: Cavity flow. Re 3200. Velocity profiles at mid-vertical and horizontal lines..... 24
Figure 11: Cavity flow. Re 10000. Velocity profiles at mid-vertical and horizontal lines..... 25
Figure 12: 2D tunnel cross-section sketch 26
Figure 13: Converted 2D tunnel cross-section..... 26
Figure 14: Final CATIA Outcome 2D Cylinder in a Tunnel..... 27
Figure 15: 2D Flow over a Cylinder Final Mesh Outcome 28
Figure 16: 2D Flow around a Circular Cylinder @ Re=100 Streamline Visualization..... 31
Figure 17: 2D Cylinder Lift and Drag Coefficient plot Re=100 33
Figure 18: 2D Cylinder Strouhal Number Re=100..... 33
Figure 19: Final CATIA Outcome of 3D Cylinder in a Tunnel 34
Figure 20: 3D Flow over a Cylinder Final Mesh Outcome 35
Figure 21: 3D Flow around a Circular Cylinder @ Re=100 Streamline Visualization..... 38
Figure 22: 3D Cylinder Lift and Drag Coefficient plot Re=100 39
Figure 23: 3D Cylinder Strouhal Number Re=100..... 40

LIST OF TABLES

Table I: Computational Condition at Different Reynolds number 21
Table II: Computational Condition for 2D Flow around a Circular Cylinder at Re 100.....29
Table III: Comparison of Results for 2D Flow around a Circular Cylinder at Re 100.....33
Table IV: Computational Condition for 3D Flow around a Circular Cylinder at Re 100 35
Table V: Comparison of 3D Flow Results.....40

1. INTRODUCTION

1.1.DESCRIPTION OF THE VISCOUS FLOW PROBLEMS

The main aim of this project is to show the interaction between fluid viscosity and a body or cavity. In this project, ANSYS Fluent software is used to model the flow problems below.

- 2D lid driven cavity flow.
- 2D flow around a cylinder for Re =100.
- 3D flow around a cylinder for Re =100.

Summary description of the above flow problems are given below.

1.1.1. 2D Lid Driven Cavity Flow

For the 2D lid driven cavity flow problem, we are required to present the ANSYS Fluent CFD analysis results for flows at different Reynolds number and developed in a lid driven square cavity.

- Expected Results
  - Steady state flow visualization at different Reynolds numbers.
  - U component of velocity along the mid vertical line (Y vs U) at different Reynolds numbers.
  - V component of velocity along the mid horizontal line (V vs x) at different Reynold numbers.
  - Comparison of ANSYS Fluent results with results provided by the scientific paper.

1.1.2. 2D Flow Around Circular Cylinder For Re =100

In the 2D flow around a circular cylinder, we are required to present the ANSYS Fluent CFD analysis results for flow around a circular cylinder at different time progression in a 2D channel and subjected to fluid flow at Reynolds number = 100.

➢ Expected Results

- Graph of change in Lift and Drag coefficient with respect to time (C_l & C_d vs Time).
- Flow visualization at different times of flow development.
- Mean drag coefficient value.
- RMS value of fluctuating lift and drag coefficient.
- Strouhal number.
- Comparison of ANSYS Fluent results with results provided by the scientific paper and experimentation.

1.1.3. 3D Flow Around Circular Cylinder For Re =100

The difference between the 2D and 3D analysis is that the circular cylinder is placed in a 3D box with the length of the cylinder spanning from one end of the box to the other and subjected to fluid flow at Reynolds number = 100. **The goal of doing the 3D analysis is to check the flow interaction effect between the side walls and the cylinder**. Note: This interaction is neglected in 2d analysis

➢ Expected Results

- Same results as 2D but with 3D flow visualisation

1.2. LITERATURE REVIEW OF PAST CONTRIBUTIONS

1.2.1. Use of Finite Element Modified Method of Characteristics for the Navier–Stokes Equations [1].

Dr. Alejandro Allievi and Dr. Rodolfo Bermejo [1] in their paper titled above used an algorithm based on **FMMC (Finite element modified method of characteristics) to solve convection–diffusion, Burgers and unsteady incompressible Navier–Stokes equations** for laminar flow problems like Navier–Stokes solution of lid-driven cavity flow at relatively high Reynolds numbers, Navier–Stokes solution of flow around a circular cylinder at *Re.* =100, Convection–diffusion equation, Gaussian hill in a uniform rotating field and Burgers equations with viscosity.

Their Implementation of the FMMC method was **based strictly on the Lagrangian description of the flow** where each mesh-point was associated with a fluid particle at time t_0 and traced at Subsequent times from t_1 to t_n as the flow progresses. Their use of this pure

Lagrangian approach over the conventional time stepping Eulerian schemes gave them the advantage of numerical stability and absence of convective terms.

Their numerical results for the 2D lid driven cavity flow and 2D flow over a circular cylinder will be used in our project to verify our ANSYS results.

1.2.2. Ghia et Al [2], Koseff and Street [3] [4].

J.R. Koseff and R.L. Street [3], used **experimentation** while U. Ghia, K.N. Ghia and C.T. Shin [2], used **analytical methods (solving Navier–Stokes equations with a multigrid method)** to visualize the flow in a lid driven cavity at high Reynolds numbers.

Again, Dr. Alejandro Allievi and Dr. Rodolfo Bermejo [1] used their results to verify their numerical results on the flow in a lid driven cavity and we will also use their results in our project to verify our results.

1.2.3. The Experimental Determination Effects Of Waves On Vortex Shedding From Cylinders [5]

R. H. Arkell and J. M. R. Graham [5] carried out investigations both numerically and by experiment into the effects of an in-line combination of mean flow and free surface waves on the shedding of vortices behind a circular cylinder and the subsequent long term development of the wake.

Dr. Alejandro Allievi and Dr. Rodolfo Bermejo [1] used their results to verify their numerical results on the flow over circular cylinder and we will also use their results in our project to verify our results.

1.2.4. Benque´ et al [6], Douglas and Russell and Pironneau [7].

The above researchers were **among the first to combine finite elements and MMC for the solution of the Navier–Stokes.** They used an L2-projection on the finite element space and the solution of the diffusion in the evaluation of the position of the fluid particles at the foot of the characteristic.

Dr. Alejandro Allievi and Dr. Rodolfo Bermejo [1] in their work, substituted the L2-projection at the position of the fluid particles at t_n by the finite element interpolation using the basic functions of the velocity. They were able to achieve this better alternative by developing their own search–locate algorithm.

2. THEORY, FUNDAMENTAL EQUATIONS AND BOUNDARY CONDITIONS USED IN FLOW MODELLING

In order to model the flow problems properly, the flow theory that best describes the flow problem is translated mathematically to create the fundamental governing equations. **Boundary conditions that apply to the flow problems are applied to the fundamental governing equations to create final equations that accurately describes the flow problem**. The final equations if they cannot be solved analytically are then discretized using numerical methods to properly model the flow. The theory, fundamental equations and boundary conditions used for the flow problems in this project are described below.

2.1. THEORY

Since the main aim of this project is to show the interaction between fluid viscosity and a body or cavity, Navier- Stokes equation is used to model the flow. **Navier – Stokes equation is used because it's the only equation that can describe how the velocity, pressure, temperature, and density of a moving fluid are related**. The equations got a bit of shape in 1827 when Navier improved on Euler work, and got its full shape in 1845, when stokes further improved on it. They are made up of time-dependent continuity equation for conservation of mass, three time-dependent conservation of momentum equations and a time-dependent conservation of energy equation. These equations are three for momentum conservation case because they are solved for x, y and z directions (3 Dimensional).

They are a group of differential equation that can technically be solved using calculus for a given flow problem but in reality are too complicated and nearly impossible to solve therefore, discretization using numerical methods are needed to get an approximate value or description of the flow problem. This gives rise to an academic branch called computational fluid dynamics (CFD). Software like ANSYS Fluent, CFX and others combine the power of high speed computing and numerical methods to very solve complex flow problems in short time. That is why we are using the above software for our project.

2.2. FUNDAMENTAL EQUATIONS

Since our flow problems involves 2D and 3D flows, the full 3D Navier- Stokes equation is need. The 3D Navier – Stokes equation describing viscous unsteady compressible flow is [8] [9]

$$\rho\left(\frac{Du}{Dt}\right) = -\frac{\partial p}{\partial x} + \mu\left(\frac{\partial^2 u}{\partial x^2} + \frac{\partial^2 u}{\partial y^2} + \frac{\partial^2 u}{\partial z^2}\right) + \mu\frac{1}{3}\frac{\partial}{\partial x}\left(\frac{\partial u}{\partial x} + \frac{\partial v}{\partial y} + \frac{\partial w}{\partial z}\right) + \rho g_x \quad (1)$$

$$\rho\left(\frac{Dv}{Dt}\right) = -\frac{\partial p}{\partial y} + \mu\left(\frac{\partial^2 v}{\partial x^2} + \frac{\partial^2 v}{\partial y^2} + \frac{\partial^2 v}{\partial z^2}\right) + \mu\frac{1}{3}\frac{\partial}{\partial y}\left(\frac{\partial u}{\partial x} + \frac{\partial v}{\partial y} + \frac{\partial w}{\partial z}\right) + \rho g_y \quad (2)$$

$$\rho\left(\frac{Dw}{Dt}\right) = -\frac{\partial p}{\partial z} + \mu\left(\frac{\partial^2 w}{\partial x^2} + \frac{\partial^2 w}{\partial y^2} + \frac{\partial^2 w}{\partial z^2}\right) + \mu\frac{1}{3}\frac{\partial}{\partial z}\left(\frac{\partial u}{\partial x} + \frac{\partial v}{\partial y} + \frac{\partial w}{\partial z}\right) + \rho g_z \quad (3)$$

Since the fluid used in our flow problem is **assumed incompressible**, the Navier –Stokes equation becomes;

Note 1: $\frac{\mu}{\rho} = \nu$

Note 2: g = Body force per unit mass or force density, u = velocity, p = pressure, ν =kinematic viscosity, μ = dynamic viscosity, ρ =Density

Note 2: Body force per unit mass on one side, the equation becomes

$$\left(\frac{Du}{Dt}\right) - \nu\left(\frac{\partial^2 u}{\partial x^2} + \frac{\partial^2 u}{\partial y^2} + \frac{\partial^2 u}{\partial z^2}\right) + \frac{1}{\rho}\frac{\partial p}{\partial x} = g_x \quad (4)$$

$$\left(\frac{Dv}{Dt}\right) - \nu\left(\frac{\partial^2 v}{\partial x^2} + \frac{\partial^2 v}{\partial y^2} + \frac{\partial^2 v}{\partial z^2}\right) + \frac{1}{\rho}\frac{\partial p}{\partial y} = g_y \quad (5)$$

$$\left(\frac{Dw}{Dt}\right) - \nu\left(\frac{\partial^2 w}{\partial x^2} + \frac{\partial^2 w}{\partial y^2} + \frac{\partial^2 w}{\partial z^2}\right) + \frac{1}{\rho}\frac{\partial p}{\partial z} = g_z \quad (6)$$

- **Converting to Frame Invariant Form** [8]

$$\frac{Du}{Dt} - \nu\Delta\mathbf{u} + \nabla\mathbf{p} = g_x \quad (8)$$

$$\frac{Dv}{Dt} - \nu\Delta\mathbf{v} + \nabla\mathbf{p} = g_y \quad (9)$$

$$\frac{Dw}{Dt} - \nu\Delta\mathbf{w} + \nabla\mathbf{p} = g_z \quad (10)$$

- **Applying Initial and Boundary conditions on the frame invariant form in x direction only** [1]

Let $\Omega \subset R^d$ (d= 2 or 3) be an open bounded domain with boundary Γ

And, assume that $\Gamma = \Gamma_1 \cup \Gamma_2$ and $\Gamma_1 \cap \Gamma_2$. Now,

At x=0 and t=t_0 (0, T),

$$\nabla\cdot\mathbf{u} = 0 \quad (11)$$

At the initial condition,

$$u(x,0) = u_0 x \quad (12)$$

At the boundary condition,

$$u(x,t) = g_1(x,t)\ on\ \Gamma 1 \quad (13)$$

$$-pn + \nu\frac{\partial u}{\partial n} = g_2(x,t)\ on\ \Gamma 2 \quad (14)$$

Where **n** is the outward unit normal to the boundary.

Note 4: $\frac{Du}{Dt} = \frac{\partial u}{\partial t} + \mathbf{u}.\nabla\mathbf{u}$ Is the material derivative of u and it measures the rate of change of u as seen by an observer moving with the fluid particles.

2.3.FLOW PROBLEMS BOUNDARY CONDITIONS

As stated earlier, the boundary conditions that apply to the flow problems are applied to the fundamental governing equations to create final equations that accurately describes the flow problem. The different boundary conditions that apply to each flow problem is described below.

2.3.1. 2D lid driven cavity flow.

$$At\ x = 0, y \neq 0\ , U = V = 0\ \left(no\ slip\ boundary\ Condition\ (wall)\right)$$

$$At\ x = x_{max}, y \neq 0\ , U = V = 0\ (no\ slip\ boundary\ Condition\ (wall))$$

$$At\ x \neq 0, y = y_{min}\ , U = V = 0\ (no\ slip\ boundary\ Condition\ (wall))$$

$$At\ x \neq 0, y = y_{max}\ , U = U_{max} = \frac{1m}{s}, V = 0$$

$$At\ x \neq 0, y \neq y_{max}\ \ and\ \ t = 0, U = V = 0$$

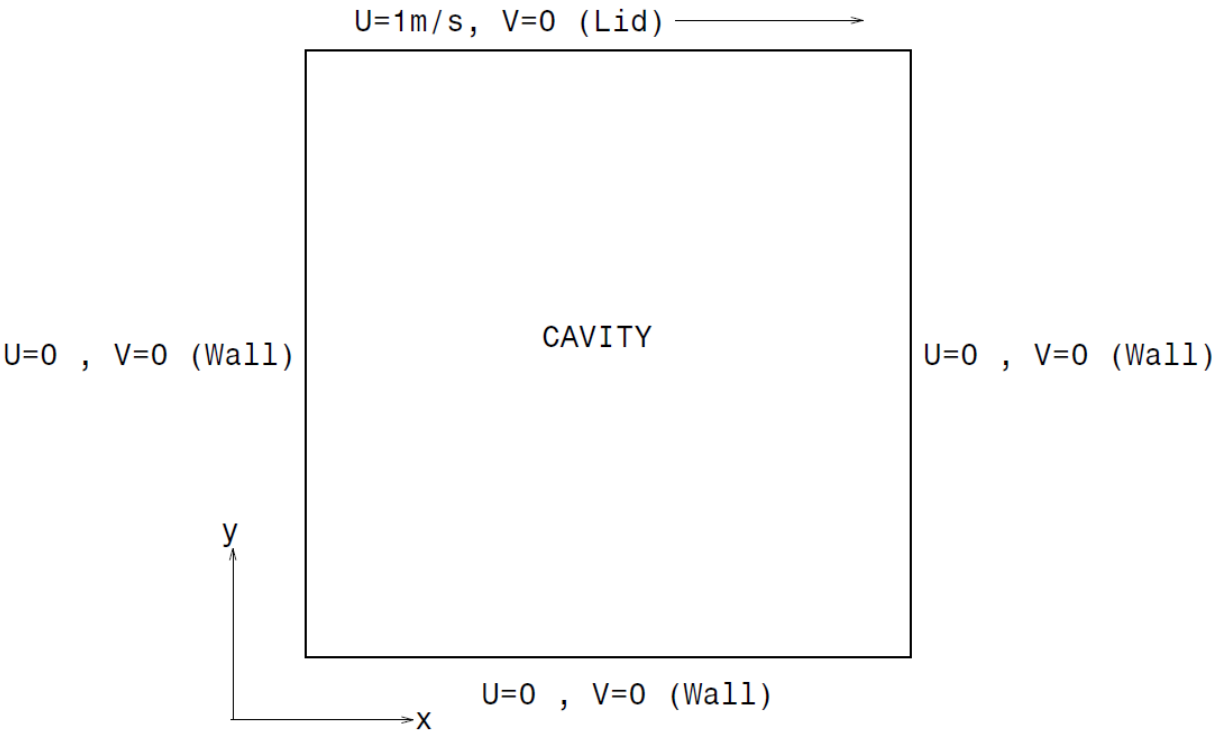

Figure 1: 2D Lid Driven Cavity Boundary Condition Diagram

- Analysis Assumptions and Parameter Description.

For the lid driven cavity flow,

Characteristic length = 1m and U= 1m/s

We know that Reynolds Number $\boldsymbol{Re} = \frac{\rho \boldsymbol{UD}}{\mu} = \frac{\boldsymbol{UD}}{\boldsymbol{\nu}}$ **(15)**

Where $\frac{\mu}{\rho} = \boldsymbol{\nu}$

Substituting the above values in equation 15,

$$\boldsymbol{Re} = \frac{\mathbf{1}}{\boldsymbol{\nu}} = \frac{\rho}{\mu} \quad \textbf{(16)}$$

ρ Is constant because the fluid is assumed incompressible therefore to get a predetermined value of Reynold number, dynamic viscosity value will have to change. This gives.

$$\mu = \frac{\rho}{\boldsymbol{Re}} \quad \textbf{(17)}$$

The flow is analysed for two cases (**Note**: density $\rho = 1\text{kg/m}^3$)

- Case 1: for Re = 3200,

$$\mu = \frac{\rho}{\boldsymbol{Re}} = \frac{\mathbf{1}}{\mathbf{3200}} = \mathbf{0.0003125}\boldsymbol{Ns/m^2} \quad \textbf{(18)}$$

- Case 2: for Re = 10000,

$$\mu = \frac{\rho}{\boldsymbol{Re}} = \frac{\mathbf{1}}{\mathbf{10000}} = \mathbf{0.0001}\boldsymbol{Ns/m^2} \quad \textbf{(19)}$$

2.3.2. 2D flow around a circular cylinder for Re =100.

$$At\ x \neq 0, y = 0\ , U = V = 0\ \left(no\ slip\ boundary\ Condition\ (wall)\right)$$

$$At\ x \neq 0, y = y_{max}\ , U = V = 0\ (no\ slip\ boundary\ Condition\ (wall))$$

$$At\ x = 0, y = \frac{y}{2}\ and\ \ U = U_{max}$$

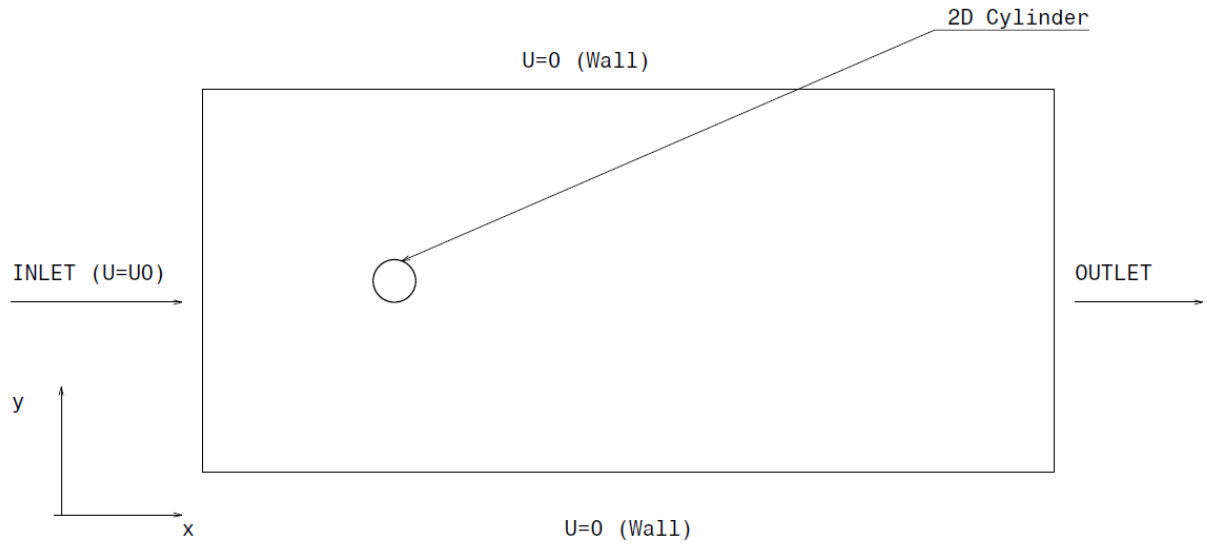

Figure 2: 2D Flow around a Cylinder Boundary Condition Diagram

- Analysis Assumptions and Parameter Description.

For this flow problem Re is kept at 100 and,

$$\boldsymbol{Re} = \frac{\boldsymbol{\rho UD}}{\mu} \qquad \textbf{(20)}$$

D = Characteristic Diameter = 1m

Assume Velocity U =1m/s then,

$$\mu = \frac{\boldsymbol{\rho UD}}{\boldsymbol{Re}} \qquad \textbf{(21)}$$

$$\mu = \frac{\mathbf{1 * 1 * 1}}{\mathbf{100}} = \mathbf{0.01 Ns/m^2}$$

2.3.3. 3D flow around a circular cylinder for Re =100.

$At\ x \neq 0, y \neq 0\ , z = 0, \quad U = V = 0\ (no\ slip\ boundary\ Condition\ (wall))$

$At\ x \neq 0, y \neq 0\ , z = z_{max}, \quad U = V = 0\ (no\ slip\ boundary\ Condition\ (wall))$

$At\ x \neq 0, y = 0\ , z \neq 0, \quad U = V = 0\ (no\ slip\ boundary\ Condition\ (wall))$

$At\ x \neq 0, y = y_{max}\ , z \neq 0, \quad U = V = 0\ (no\ slip\ boundary\ Condition\ (wall))$

$At\ x = 0, y = \frac{y}{2}\ , z = \frac{z}{2}, \quad U = Umax$

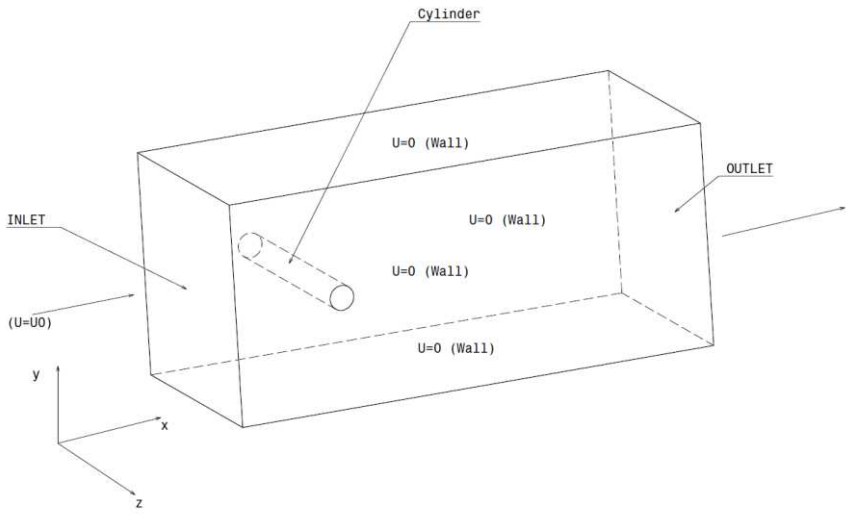

Figure 3: 3D Flow around a Cylinder Boundary Condition Diagram

- Analysis Assumptions and Parameter Description.

For this flow problem Re is kept at 100 and,

$$\boldsymbol{Re} = \frac{\boldsymbol{\rho UD}}{\mu} \tag{22}$$

$D = Characteristic\ Diameter = 1m$

Assume Velocity U = 1m/s then,

$$\mu = \frac{\boldsymbol{\rho UD}}{\boldsymbol{Re}} \tag{23}$$

$$\mu = \frac{\mathbf{1*1*1}}{\mathbf{100}} = \mathbf{0.01}\boldsymbol{Ns/m^2}$$

3. NUMERICAL METHODS AND SOLUTION ALGORITHM USED

When using ANSYS fluent to model a flow problem, there are two solver technologies that exist.

- Pressure Based Solver Algorithms [10]

This solver based algorithms is used mostly for incompressible and mildly compressible flow problems and is **subdivided into segregated and coupled algorithms**. The pressure-based solver uses a solution algorithm where, the governing mass, momentum and sometimes energy continuity equations are solved sequentially while, pressure-based coupled algorithm solves a coupled system of equations comprising the momentum equations and the pressure-based continuity equation.

- Density Based Solver Algorithms [10]

This solver based algorithms is used mostly for high speed compressible flow problems and is also **subdivided into implicit and explicit algorithms.**

3.1. NUMERICAL METHOD USED

3.1.1. Overall Discretization Method

- Temporal Discretization [10]

For transient simulations, the governing equations are be discretized in both space and time. The spatial discretization for the time-dependent equations is identical to the steady-state case. Temporal discretization involves the integration of every term in the differential equations over a time step Δt. The integration of the transient terms is straightforward, as shown below.

A generic expression for the time evolution of a variable φ is given by,

$$\frac{\partial \varphi}{\partial t} = F(\varphi) \qquad (24)$$

Where the function F incorporates any spatial discretization. If the time derivative is discretized using **backward differences**, the first-order accurate temporal discretization is given by

$$\frac{\varphi^{n+1}-\varphi^{n}}{\Delta t} = F(\varphi) \qquad (25)$$

And the second-order discretization is given by,

$$\frac{3\varphi^{n+1}-4\varphi^{n}+4\varphi^{n-1}}{2\Delta t} = F(\varphi) \quad \textbf{(26)}$$

where

φ = a scalar quantity

$n+1$ = value at the next time level, $t+\Delta t$

n = value at the current time level, t

$n-1$ = value at the previous time level, $t-\Delta t$

Once the time derivative has been discretized, a choice remains for evaluating $F(\varphi)$: in particular, which time level values of φ should be used in evaluating F.

- Implicit Time Integration [10]

One method is to evaluate $F(\varphi)$ at the future time level:

$$\frac{\varphi^{n+1}-\varphi^{n}}{\Delta t} = F(\varphi^{n+1}) \quad \textbf{(27)}$$

This is referred to as "implicit" integration since φ^{n+1} in a given cell is related to φ^{n+1} in neighbouring cells through $F(\varphi^{n+1})$:

$$\varphi^{n+1} = \varphi^{n} + \Delta t F(\varphi^{n+1}) \quad \textbf{(28)}$$

This implicit equation can be solved iteratively at each time level before moving to the next time step.

The advantage of the fully implicit scheme is that it is unconditionally stable with respect to time step size.

3.1.2. Discretization of the Momentum Equation [10]

The discretization scheme described above for a scalar transport equation is also used to discretize the momentum equations. For example, the x-momentum equation can be obtained by setting φ=u:

$$\boldsymbol{a_p u = \sum_{nb} a_{nb} u_{nb} + \sum p_f A * \hat{i} + S} \quad \textbf{(29)}$$

If the pressure field and face mass fluxes are known, can be solved in the manner outlined and a velocity field obtained. However, the pressure field and face mass fluxes are not known a prior and must be obtained as a part of the solution. There are important issues with respect to the storage of pressure and the discretization of the pressure gradient term which are addressed next.

ANSYS Fluent uses a co-located scheme, whereby pressure and velocity are both stored at cell centres. However, above requires the value of the pressure at the face between cells $C0$ and$C0$, therefore, an interpolation scheme is required to compute the face values of pressure from the cell values.

3.1.3. Discretization of the Continuity Equation [10]

$$\boldsymbol{\oint \rho \vec{v}.d\vec{A} = 0} \quad \textbf{(30)}$$

Above equation may be integrated over the control volume to yield the following discrete equation

$$\boldsymbol{\sum_f^{N_{faces}} J_f A_f = 0} \quad \textbf{(31)}$$

Where J_f is the mass flux through face$f$, ρv_n.

In order to proceed further, it is necessary to relate the face values of velocity, $\overrightarrow{J_f}$, to the stored values of velocity at the cell centers. Linear interpolation of cell-centered velocities to the face results in unphysical checkerboarding of pressure. ANSYS Fluent uses a procedure similar to that outlined by Rhie and Chow to prevent checkerboarding. The face value of velocity is not averaged linearly; instead, momentum-weighted averaging, using weighting factors based on the $\overrightarrow{v_n}$ coefficient from Momentum equation, is performed. Using this procedure, the face flux,

J_f, may be written as.

$$\boldsymbol{J_f = \rho_f \frac{a_{p,c0}v_{n,c0}+a_{p,c1}v_{n,c1}}{a_{p,c0}+a_{p,c1}} + d_f\left((p_{c0} + (\nabla p)_{c0} * \overrightarrow{r_0}) - (p_{c1} + (\nabla p)_{c1} * \overrightarrow{r_1})\right)} \quad \textbf{(32)}$$

$$\boldsymbol{= \widehat{J_f} + d_f(p_{c0} - p_{c1})} \quad \textbf{(33)}$$

where p_{c0}, p_{c1}, and $v_{n,c0}, v_{n,c0}$ are the pressures and normal velocities, respectively, within the two cells on either side of the face, and $\overrightarrow{J_f}$ contains the influence of velocities in these The term d_f is a function of $\overrightarrow{a_p}$, the average of the momentum equation a_p coefficients for the cells on either side of face f.

3.2. SOLUTION ALGORITHM USED

Form the description given in chapter two's "**Analysis Assumptions and Parameter Description",** our flow problems are based on an incompressible fluid (water) travelling at a very slow speed (1m/s maximum). From the information, pressure based solver algorithms is most suited for our flow problems.

3.2.1. Pressure Based Solver Algorithms [10]

Pressure-based solver uses a projection method algorithm that achieves mass conservation (continuity) of the velocity field by solving a pressure (or pressure correction) equation which is derived from the continuity and the momentum equations in such a way that the velocity field, corrected by the pressure, satisfies the continuity. These governing equations are nonlinear and coupled to one another, the solution process involves iterations wherein the entire set of governing equations is solved repeatedly until the solution converges. The solution algorithm we used is;

3.1.1.1.Pressure Based Segregated Algorithms. [10]

The pressure-based solver uses a solution algorithm where the governing equations are solved sequentially (that is, segregated from one another). Because the governing equations are nonlinear and coupled, the solution loop must be carried out iteratively in order to obtain a converged numerical solution.

In the segregated algorithm, the individual governing equations for the solution variables (for example, $u, v, w, p, T, k, \varepsilon$ and so on) are solved one after another. Each governing equation, while being solved, is "decoupled" or "segregated" from other equations, hence its name. The segregated algorithm is memory-efficient, since the discretized equations need only be stored in the memory one at a time. However, the solution convergence is relatively slow, in as much as the equations are solved in a decoupled manner.

- Step By Step Process Used By Pressure Based Segregated Algorithm To Achieve Convergence.

i. Update fluid properties (for example, density, viscosity, specific heat) including turbulent viscosity (diffusivity) based on the current solution.
ii. Solve the momentum equations, one after another, using the recently updated values of pressure and face mass fluxes.
iii. Solve the pressure correction equation using the recently obtained velocity field and the mass-flux.
iv. Correct face mass fluxes, pressure, and the velocity field using the pressure correction obtained from Step 3.
v. Solve the equations for additional scalars, if any, such as turbulent quantities, energy, species, and radiation intensity using the current values of the solution variables.
vi. Update the source terms arising from the interactions among different phases (for example, source term for the carrier phase due to discrete particles).
vii. Check for the convergence of the equations.
viii. These steps are continued until the convergence criteria are met.

➢ Flow Chart Representing The Above Steps

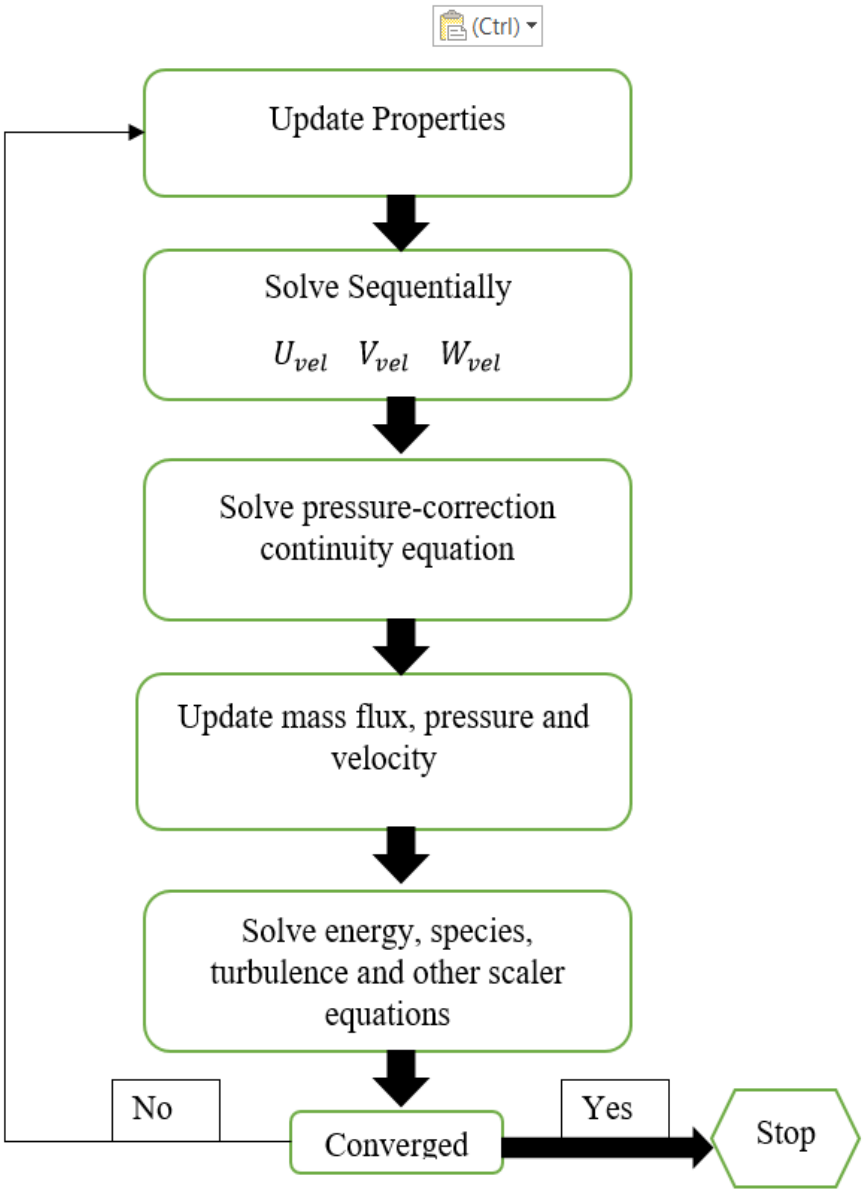

Figure 4: Flow Chart of Working Pressure Based Segregated Algorithm.

➢ Actual Pressure Based Segregated Algorithms

SIMPLE

The SIMPLE algorithm uses a relationship between velocity and pressure corrections to enforce mass conservation and to obtain the pressure field.

If the momentum equation is solved with a guessed pressure field p^*, the resulting face flux, J_f^*, computed from,

$$\boldsymbol{J_f^* = J_f^* + d_f(p_{c0}^* - p_{c1}^*)} \quad \textbf{(35)}$$

Does not satisfy the continuity equation. Consequently, a correction J_f' is added to the face flux J_f^* so that the corrected face flux, J_f

$$\boldsymbol{J_f = J_f^* + J_f'} \quad \textbf{(34)}$$

Satisfies the continuity equation. The SIMPLE algorithm postulates that J_f' be written as

$$\boldsymbol{J_f' = d_f(p_{c0}' - p_{c1}')} \quad \textbf{(36)}$$

Where p' is the cell pressure correction

The SIMPLE algorithm substitutes the flux correction equations into the discrete continuity equation to obtain a discrete equation for the pressure correction p' in the cell:

$$\boldsymbol{a_p\, p' = \sum_{nb} a_{nb} p_{nb}' + b} \quad \textbf{(37)}$$

Where the source term b is the net flow rate into the cell:

$$\boldsymbol{b = \sum_f^{N_{faces}} J_f^* A_f} \quad \textbf{(38)}$$

The pressure-correction equation may be solved using the algebraic multigrid (AMG) method. Once a solution is obtained, the cell pressure and the face flux are corrected using

$$\boldsymbol{p = p^* + \alpha_p p'} \quad \textbf{(39)}$$

$$\boldsymbol{J_f = J_f^* + d_f(p_{c0}' - p_{c1}')} \quad \textbf{(40)}$$

Here α_p is the under-relaxation factor for pressure .The corrected face flux, J_f , satisfies the discrete continuity equation identically during each iteration.

4. RESULTS

4.1. 2D LID DRIVEN CAVITY FLOW

4.1.1. Geometry Modelling

CATIA Sketcher is used to create the 2D square box sketch and CATIA Wireframe and Surface design fill function is used to convert the 2D sketch to 2D plane. The CATIA file is saved as an IGS file to be imported to ANSYS Fluent for meshing.

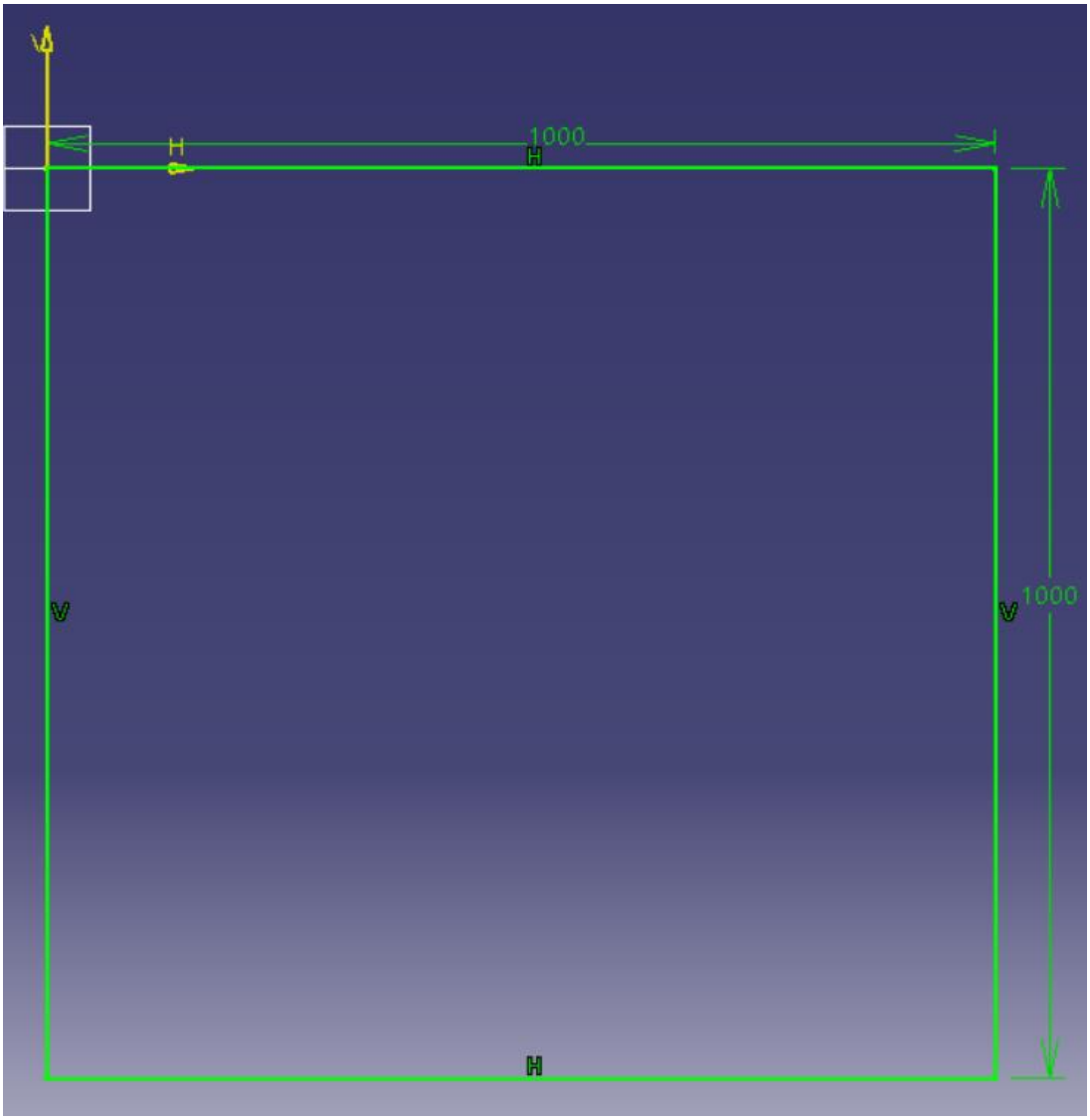

Figure 5: Sketcher 2D Box

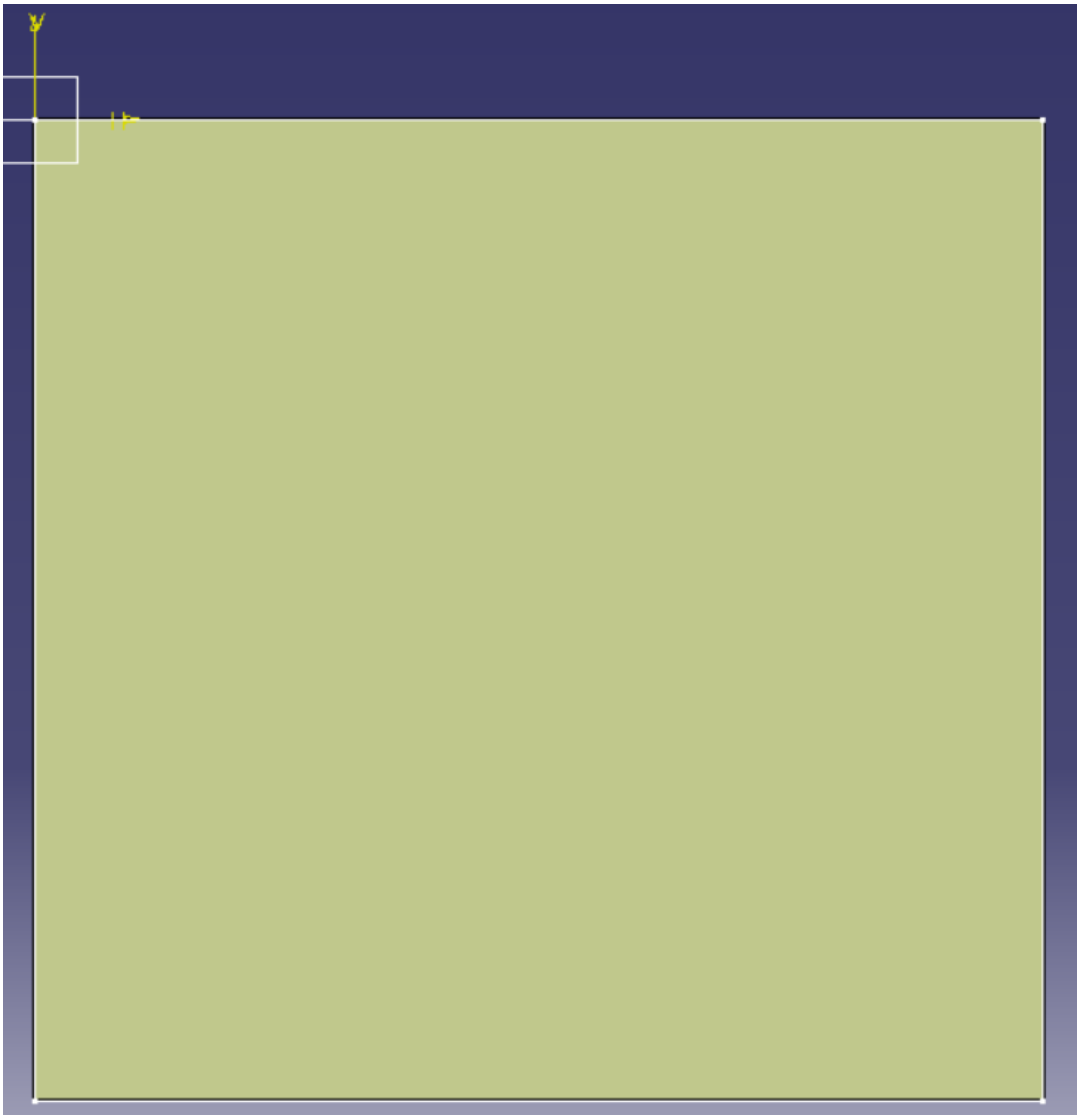

Figure 6: Converted 2D Plane

4.1.2. Geometry Meshing

For accurate results, the mesh is made in such a way that the mesh grids are concentrated at the boundaries. A Fine mesh of 120 x 100 is used for both 3200 and 10000 Reynolds numbers.

Edge sizing is inserted for the lengthwise and breadthwise edges with edge definition changed from element size to number of divisions and number of divisions is given as 120 and 100 respectively. **A double extreme end biased spacing is used with biased factor set to 12 and 10 respectively. (This helps concentrate the mesh at the edge boundaries)**

Mapped Face meshing is used to keep the mesh lines straight. The final output of the mesh is given below.

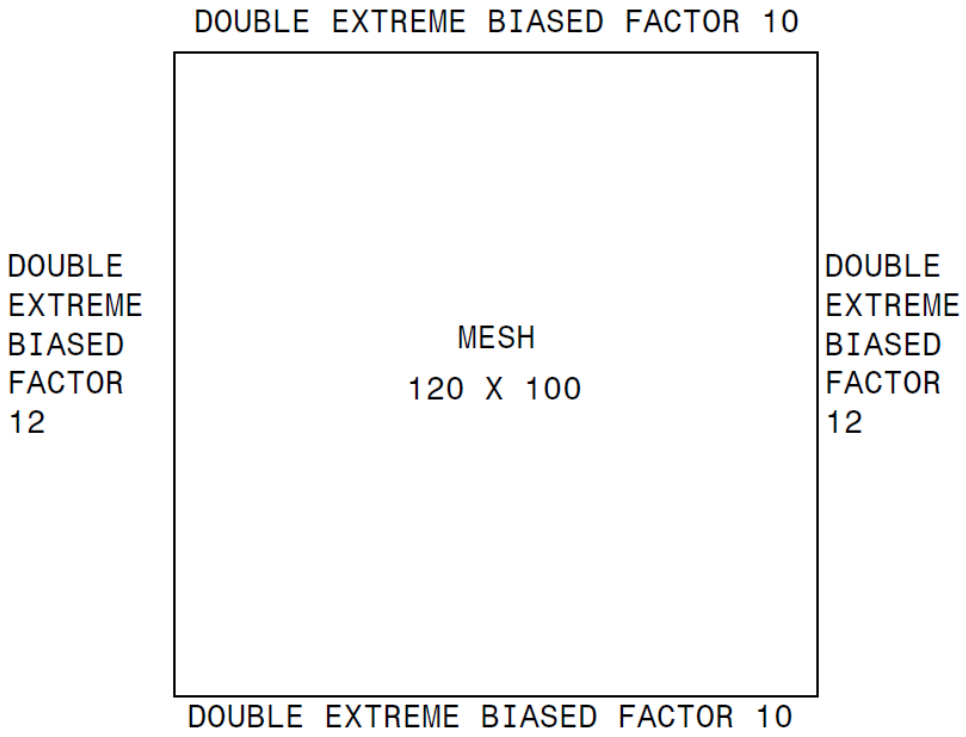

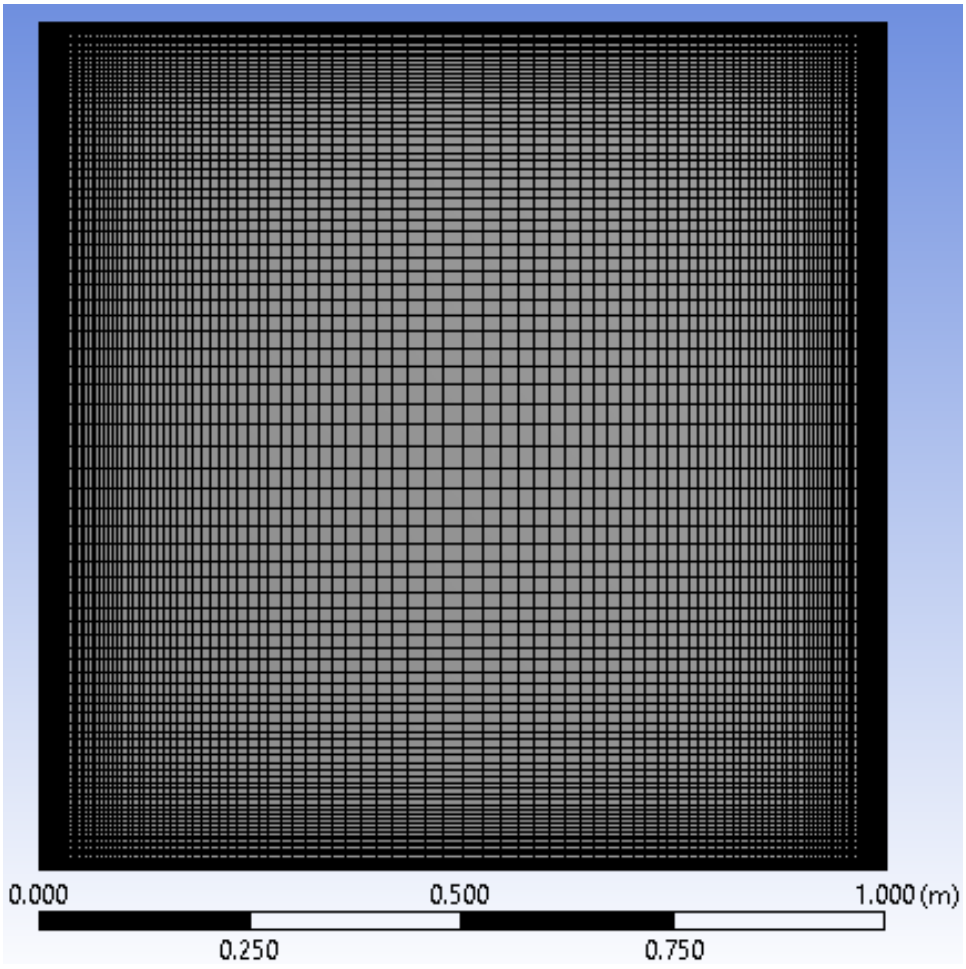

Figure 7: 2D Flow over a Cylinder Final Mesh Outcome

4.1.3. Computational Conditions

Table I: Computational Condition at Different Reynolds number

Problem No	Reynolds No	Mesh Divisions	Biased Type	Biased Factor	Nodes
1	3200	120x100	double extreme end	12x10	12221
2	10000	120x100	double extreme end	12x10	12221

4.1.4. Flow and Analysis Conditions

$$\boldsymbol{Re = \frac{1}{\nu} = \frac{\rho}{\mu}} \quad \textbf{(41)}$$

Therefore;

$$\mu = \frac{\boldsymbol{\rho}}{\boldsymbol{Re}} \quad \textbf{(42)}$$

The flow is analysed for two cases (**Note**: density $\rho = 1\text{kg/m}^3$

- Case 1: for Re = 3200,

$$\mu = \frac{\rho}{Re} = \frac{1}{3200} = \boldsymbol{0.0003125 Ns/m^2} \quad \textbf{(43)}$$

- Case 2: for Re = 10000,

$$\mu = \frac{\rho}{Re} = \frac{1}{10000} = \boldsymbol{0.0001 Ns/m^2} \quad \textbf{(44)}$$

NOTE:

- **Viscous Laminar pressure based solver** model is used for solving the above flow
- Lid velocity = 1m/s
- Time stepping method = Fixed
- Time Step Size = 1 sec
- Total number of time Steps =150
- Total Time (Total number of time Steps * Time Step Size) = 150 sec
- Max number of Iterations per time step = 20
- Data recording time interval = 5 sec

4.1.5. ANSYS Modelling Output

- Cavity Flow Streamline Visualization

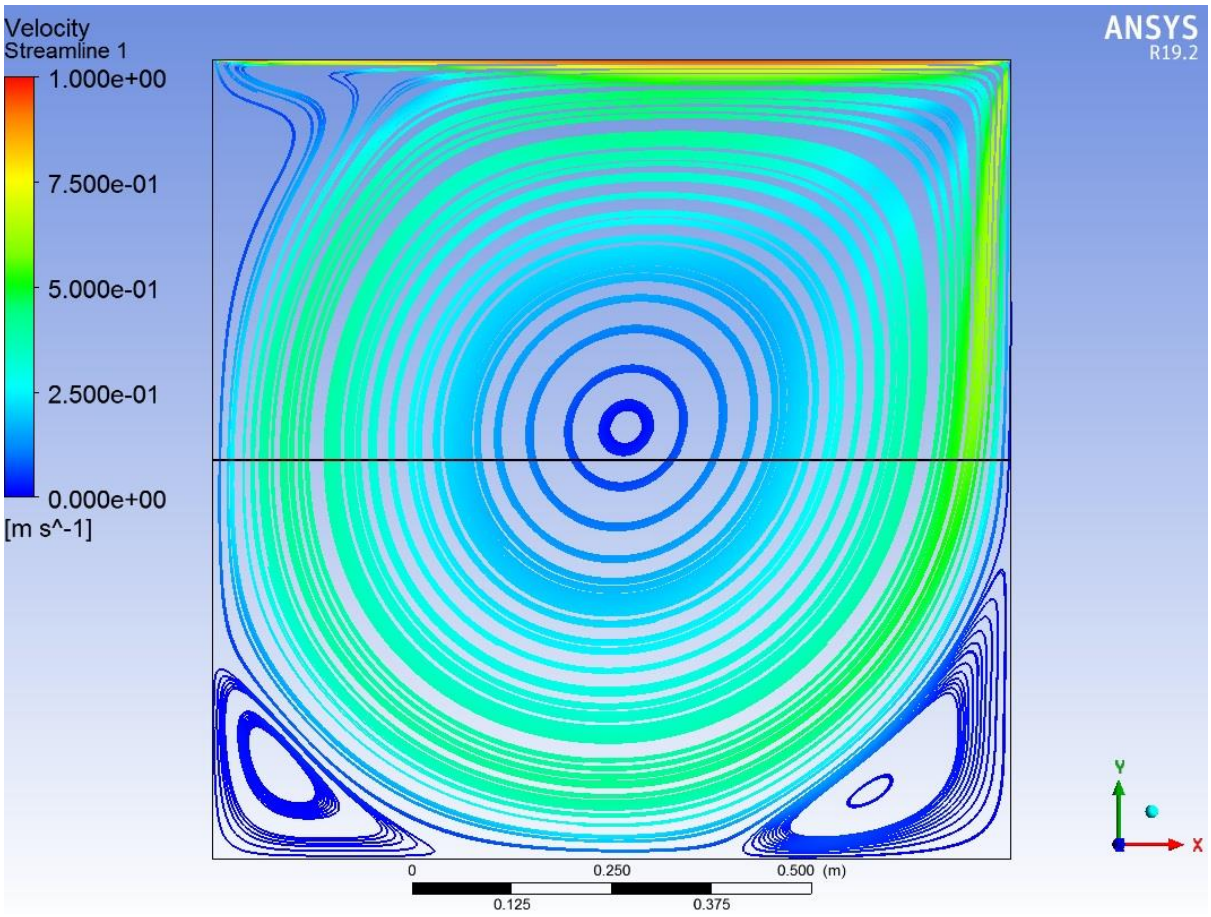

Figure 8: Cavity Flow at Re 3200

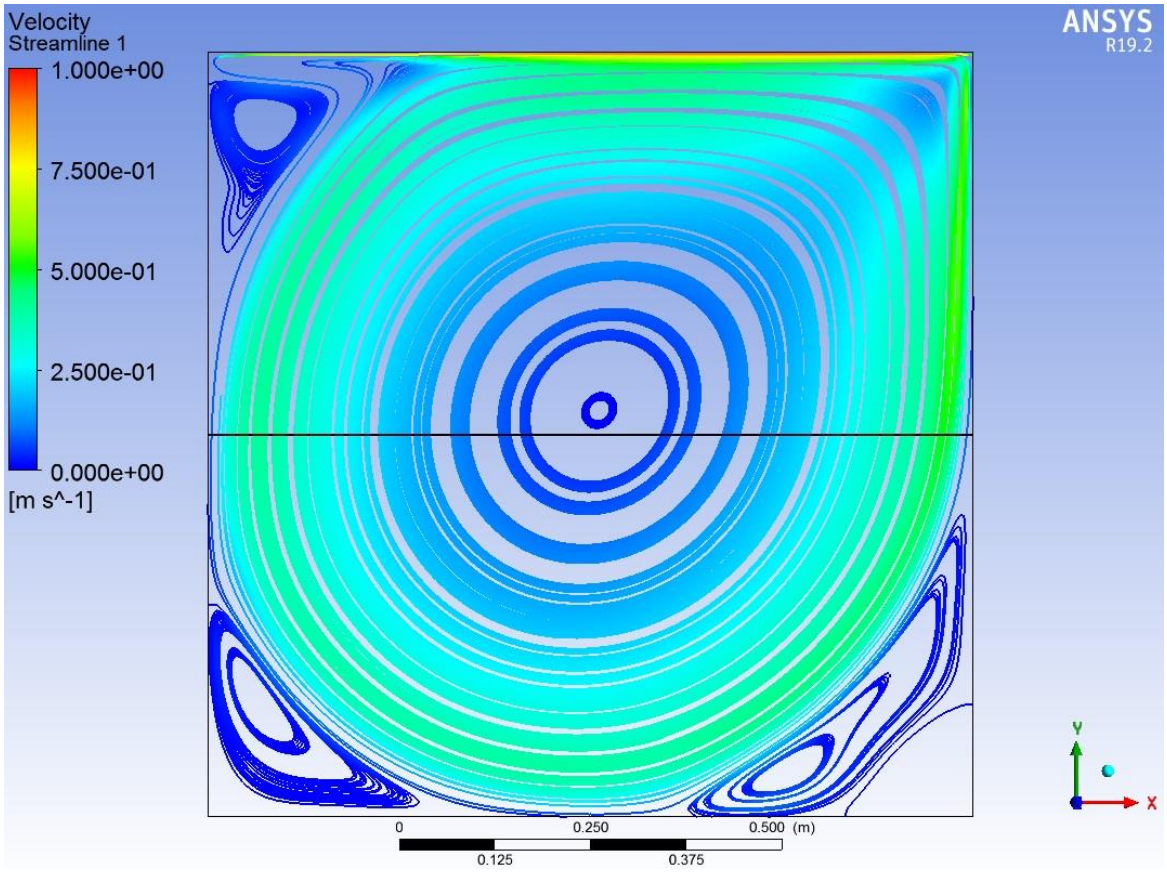

Figure 9: Cavity Flow at Re 10000

- U and V velocity Components Comparison Plots for Re= 3200 and 10000

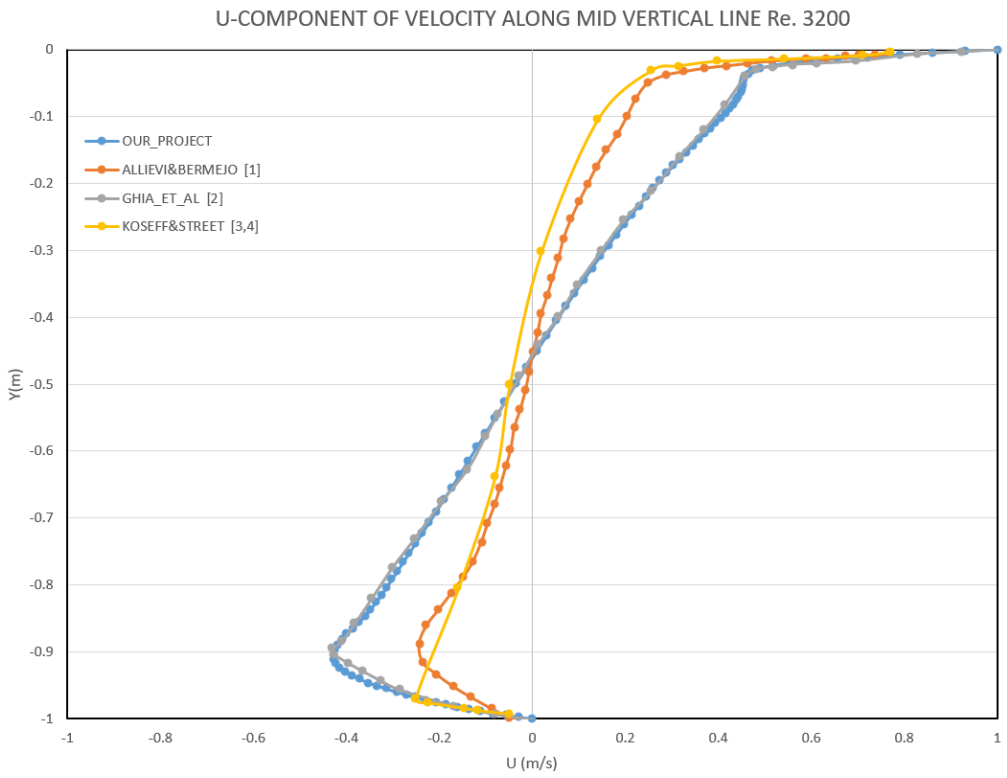

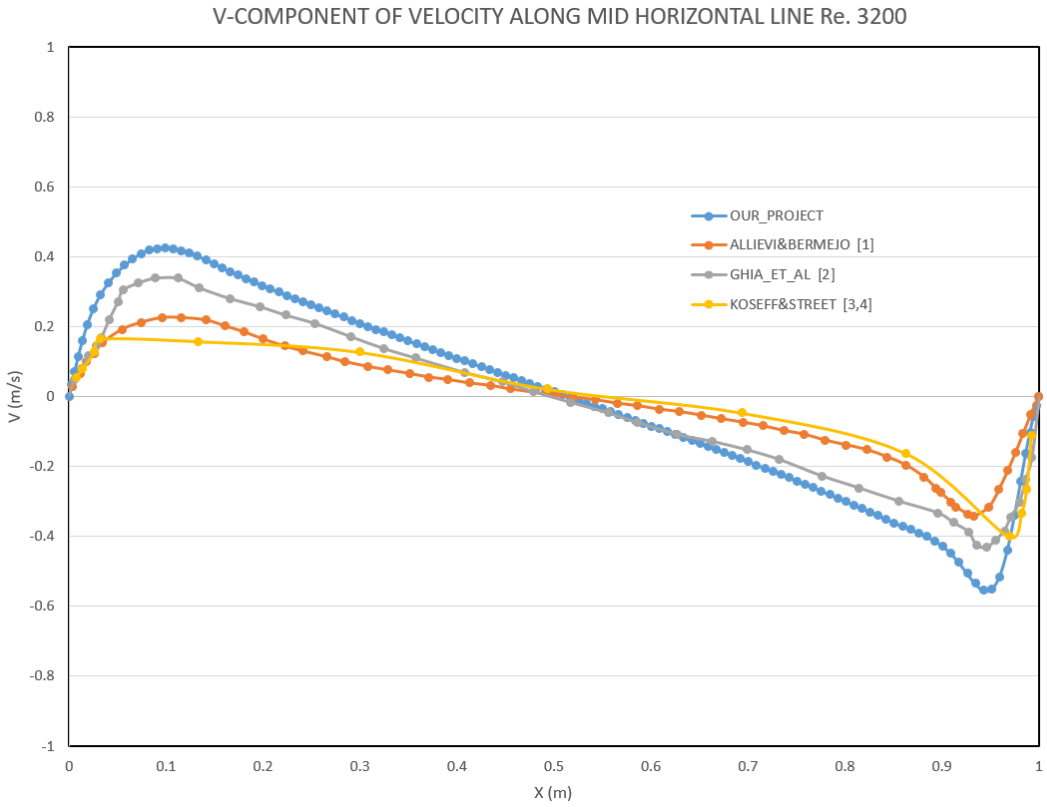

Figure 10: Cavity flow. Re 3200. Velocity profiles at mid-vertical and horizontal lines

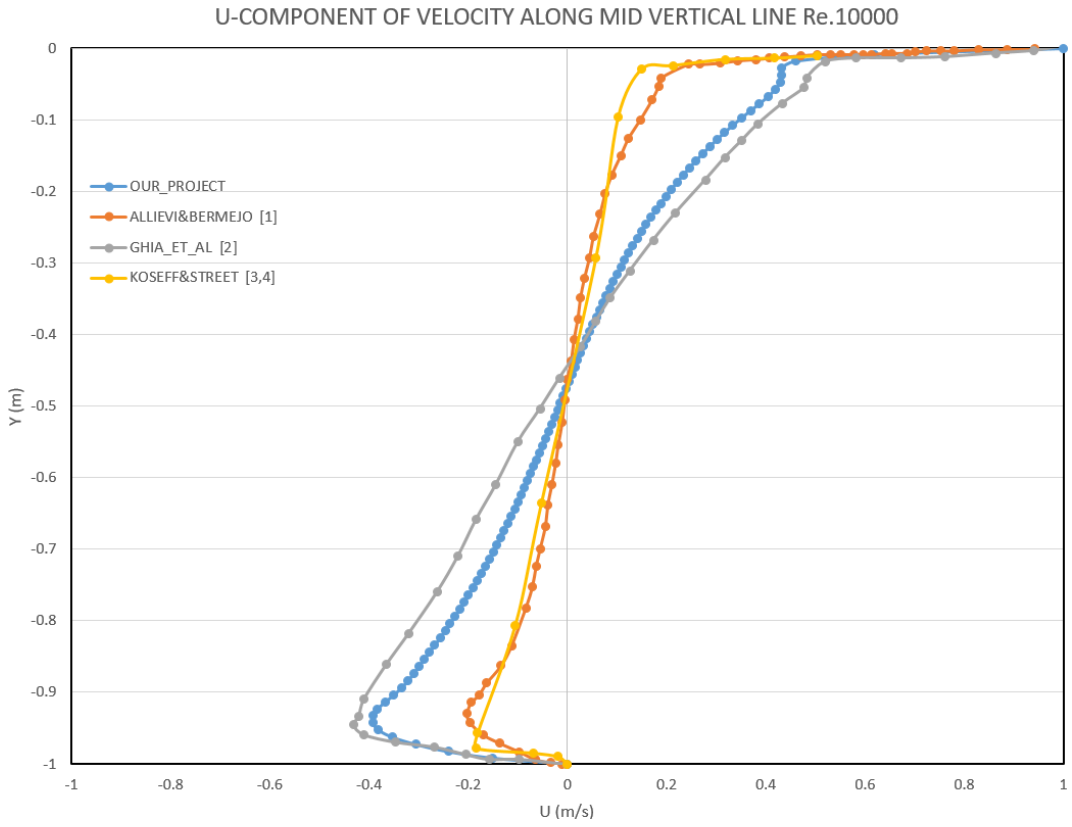

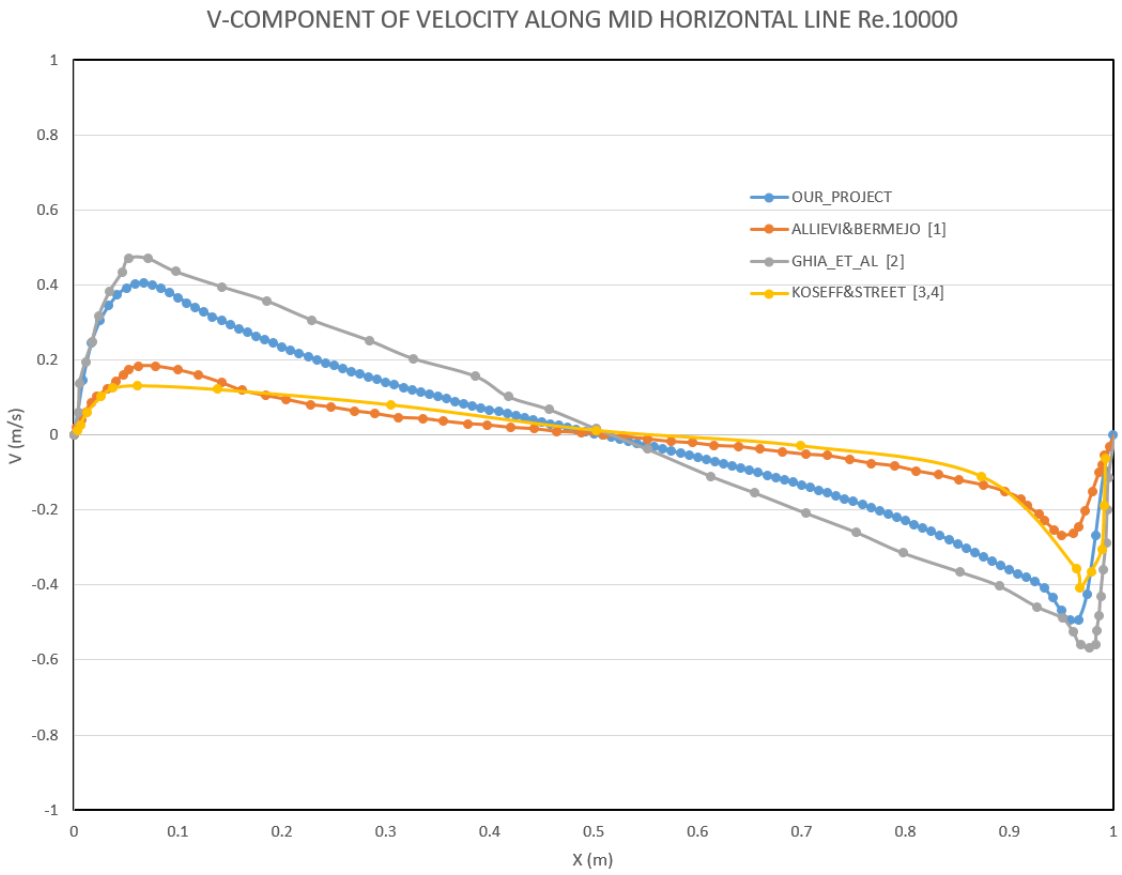

Figure 11: Cavity flow. Re 10000. Velocity profiles at mid-vertical and horizontal lines

➢ Conclusion

From the above we conclude that lid driven flow at Reynolds number 3200 has primary eddy (in centre) downstream secondary eddy (right-side down) and upstream secondary eddy (left-side down) but, at Reynolds number 10000, an additional upper stream eddy (left-side up) appears, which is a turbulent characteristic. The flow visualizations and velocity component plots along mid lines results, show a good agreement with the results published by Allievi and Bermejo [1] , Ghia et Al [2], and Koseff and Street [3] [4].

4.2. 2D Flow Around Circular Cylinder For Re =100

4.2.1. Geometry Modelling

CATIA Sketcher is used to create the 2D tunnel cross-section sketch and CATIA Wireframe and Surface design **fill function** is used to convert the 2D sketch to 2D plane. CATIA Wireframe and Surface design **split function** is used to partition the 2D plane for easy meshing to give the output below. The resulting CATIA file is saved as an IGS file to be imported to ANSYS Fluent for meshing.

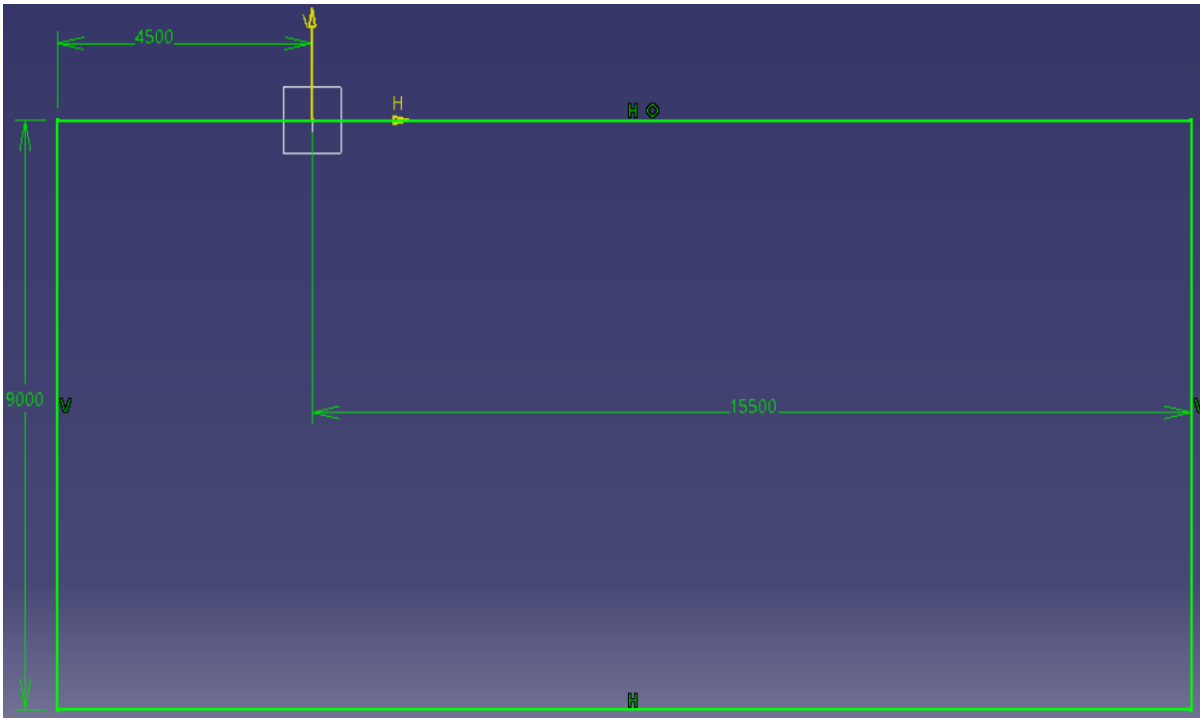

Figure 12: 2D tunnel cross-section sketch

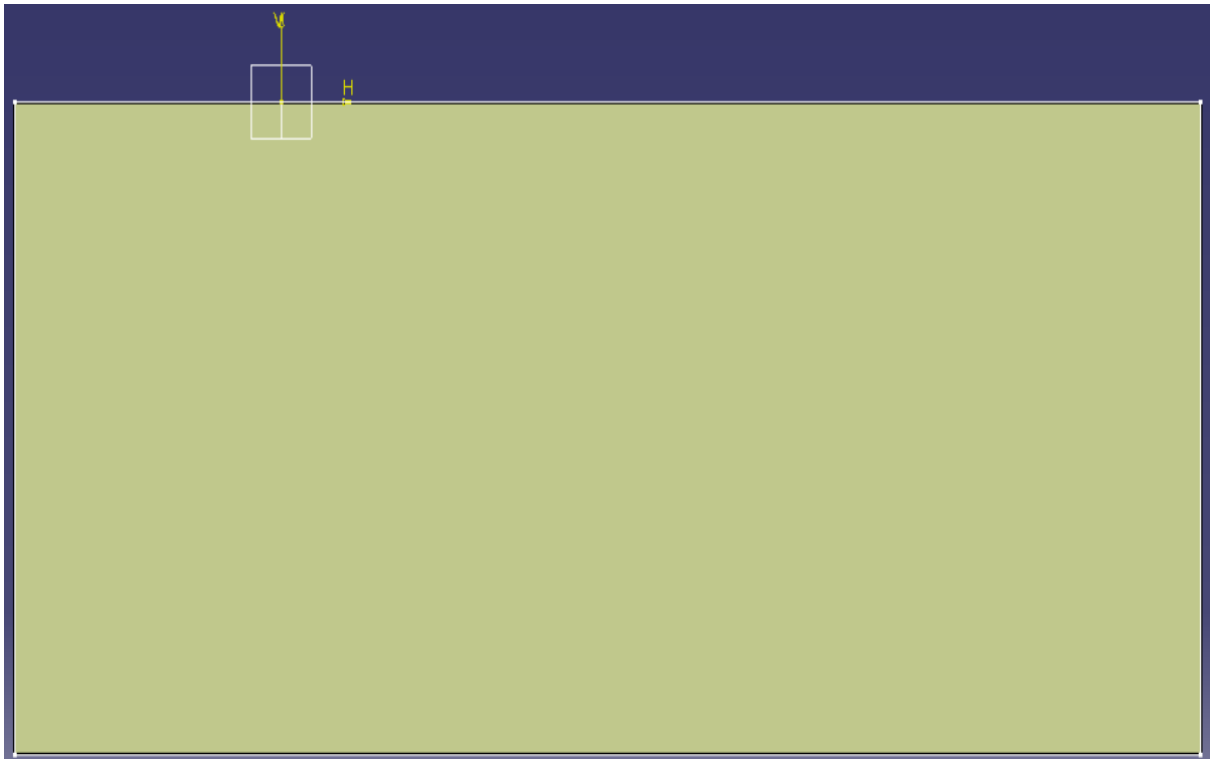

Figure 13: Converted 2D tunnel cross-section

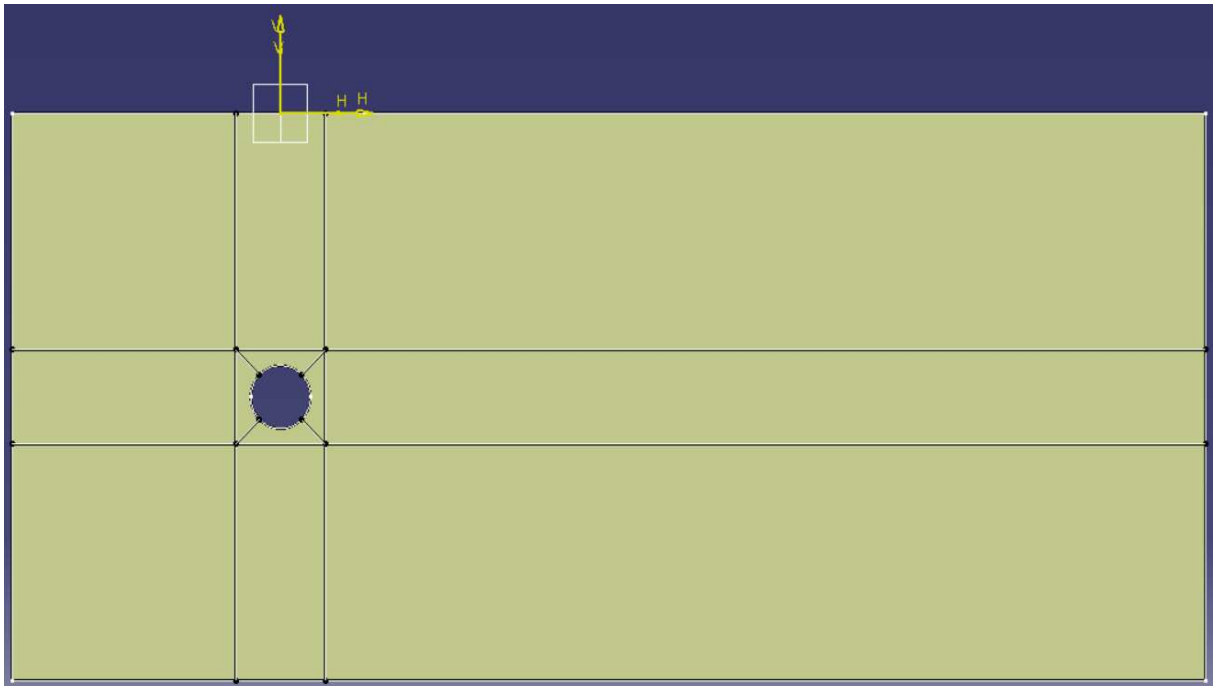

Figure 14: Final CATIA Outcome 2D Cylinder in a Tunnel

4.2.2. Geometry Meshing

For this flow problem mesh, a little complex approach is used. The 2D cylinder in a tunnel is divided into 6 sections with the cylinder in the centre as shown in the sketch. Fine mesh of $x\ X\ y$ is applied to each section of the divisions with the exception of the lines in the middle boxes that are close to the cylinder.

Edge sizing is inserted for the lengthwise and breadthwise edges of each box with edge definition changed from element size to number of divisions and number of divisions. The number of divisions given is shown in the diagram below. **A Single extreme end biased spacing is used with biased factor set in the direction of the cylinder (This helps concentrate the mesh around the cylinder bound-layer).**

- Arrow indicates direction of edge sizing with biased factor
- **middle box lines without arrow means no biased factor**
- Lines with 40 and 60 edge sizing's have biased factors of 4 and 25 respectively
- Mapped Face meshing is used to keep the mesh lines straight across all six sections. The final output of the mesh is given below.

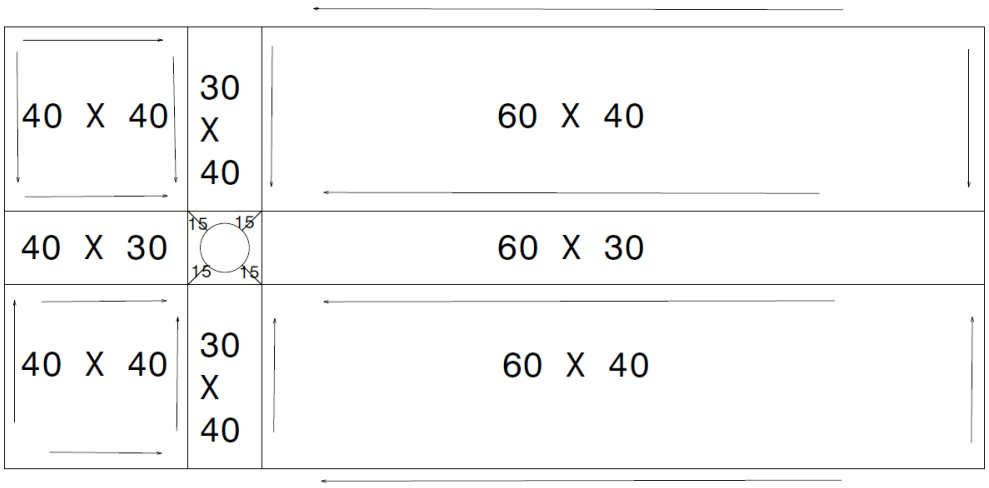

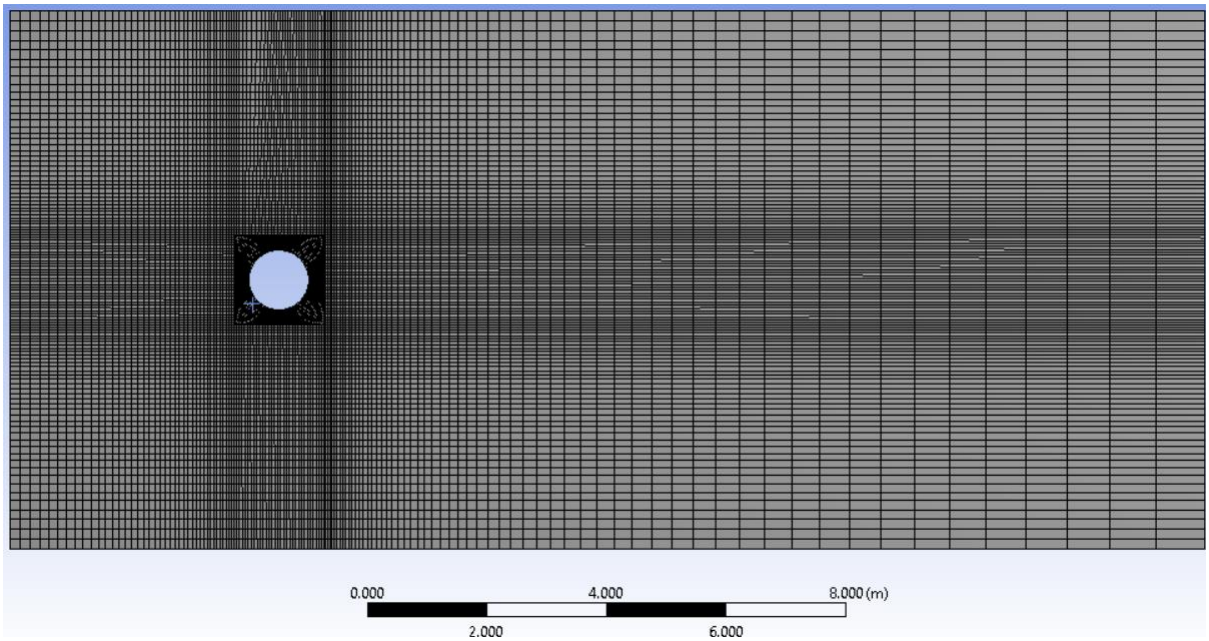

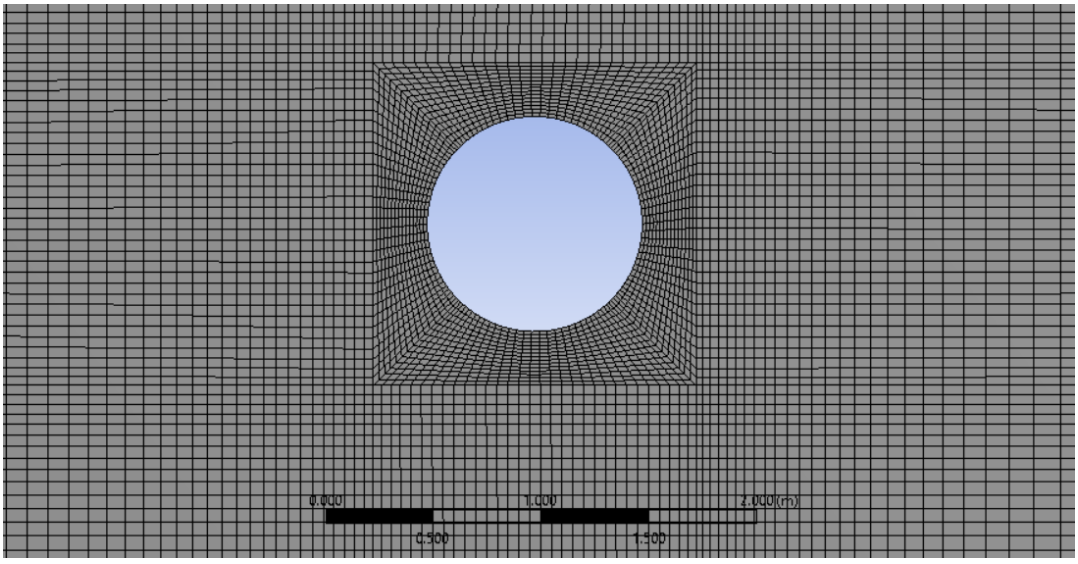

Figure 15: 2D Flow over a Cylinder Final Mesh Outcome

4.2.3. Computational Conditions

Table II: Computational Condition for 2D Flow around a Circular Cylinder at Re 100

Problem No	Reynolds No	Mesh Divisions	Biased Type	Biased Factor	Nodes
1	100	See Diagram Above	A Single extreme end biased spacing is used with biased factor set in the direction of the cylinder with exception of middle Lines	25 x4	15632

4.2.4. Flow Conditions

For this flow problem Re is kept at 100 and,

$$\boldsymbol{Re} = \frac{\boldsymbol{\rho UD}}{\mu} \qquad \textbf{(45)}$$

$D = Characteristic\ Diameter = 1m$

Density of air is = 1kg/m^2

Assume Velocity U = 1m/s then,

$$\mu = \frac{\boldsymbol{\rho UD}}{\boldsymbol{Re}} \qquad \textbf{(46)}$$

$$\mu = \frac{\mathbf{1 * 1 * 1}}{\mathbf{100}} = \mathbf{0.01 Ns/m^2}$$

NOTE:

- **Viscous Laminar pressure based solver** model is used for solving the above flow
- Flow velocity = 1m/s
- Time stepping method = Fixed
- Time Step Size = 0.5 sec
- Total number of time Steps =600
- Total Time (Total number of time Steps * Time Step Size) = 300sec
- Max number of Iterations per time step = 20
- Data recording time interval = 20 sec

4.2.5. ANSYS Modelling Output

➢ 2D Flow around a Circular Cylinder @ Re=100 Streamline Visualization

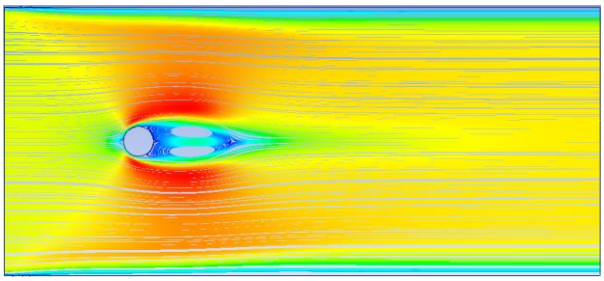

Time =10

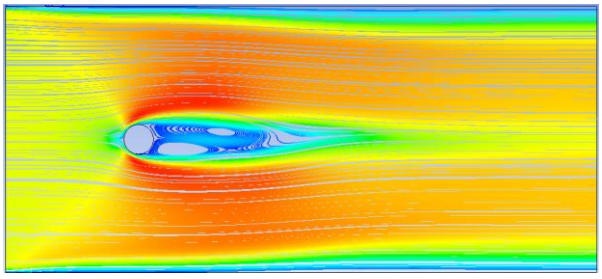

Time =20

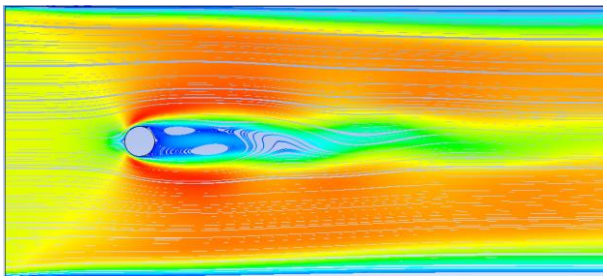

Time =30

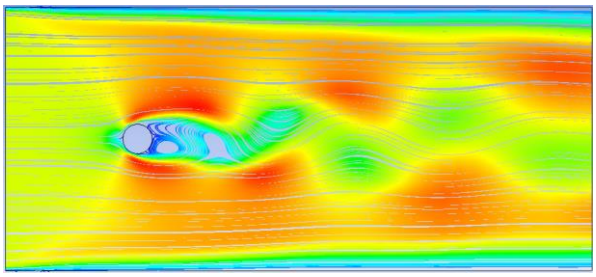

Time =40

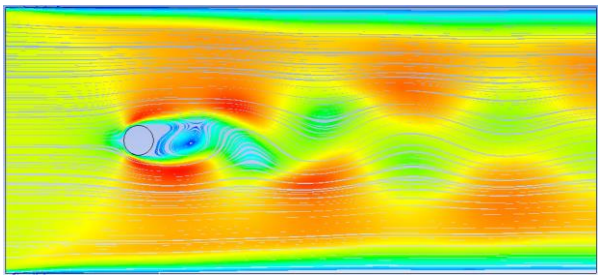

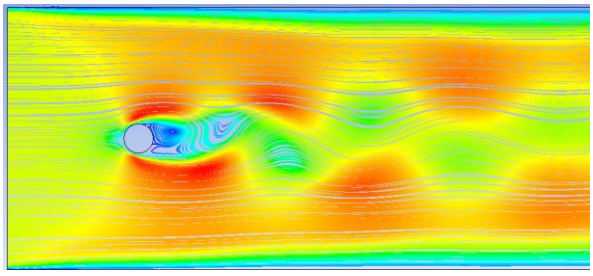

Time =50 Time =60

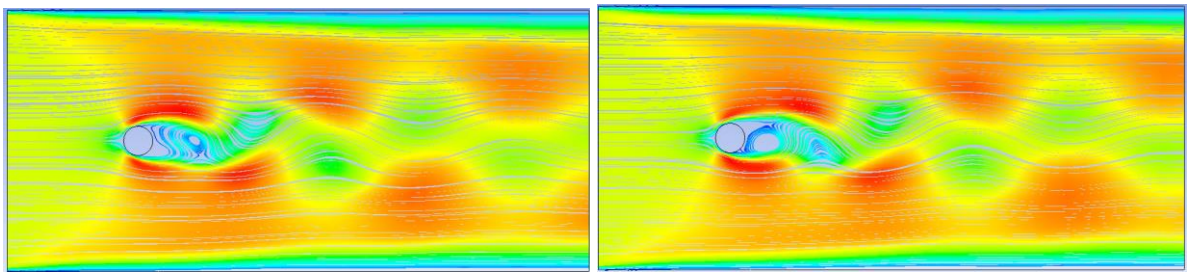

Time =70 Time =80

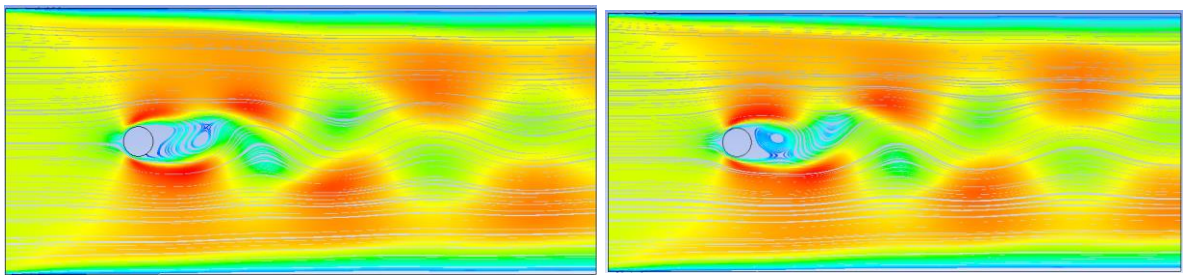

Time =90 Time =100

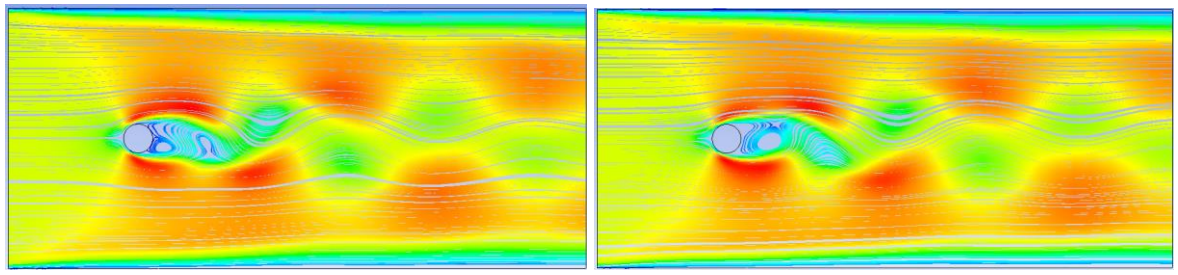

Time =110 Time =120

Figure 16: 2D Flow around a Circular Cylinder @ Re=100 Streamline Visualization

4.2.6. Conclusion With Lift and Drag Coefficient plot

- Drag Co-efficient (C_d)

Drag co-efficient is a non-dimensional number which represents the combined effect of friction drag and the pressure drag is derived by dividing drag force with dynamic pressure.

$$\boldsymbol{C_{d(Total)} = C_{d(Friction)} + C_{d(Pressure)}} \quad \textbf{(47)}$$

$$\boldsymbol{C_{d(Total)} = \frac{F_{d(Friction)}}{\frac{1}{2}\rho U_0^2 D} + \frac{F_{d(Pressure)}}{\frac{1}{2}\rho U_0^2 D}} \quad \textbf{(48)}$$

Where,

F_d = Drag Force

U_0= Free Stream Velocity

D= Cylinder Diameter

- Lift co-efficient (C_L)

Lift co-efficient is also, the ratio of lift force to the dynamic pressure.

$$C_{L(Total)} = C_{L(Friction)} + C_{L(Pressure)} \quad (49)$$

$$C_L = \frac{F_L(Friction)}{\frac{1}{2}\rho U_0^2 D} + \frac{F_L(Pressure)}{\frac{1}{2}\rho U_0^2 D} \quad (50)$$

Where,

F_L= Lift Force

- Strouhal Number (Sr)

Is a dimensionless number that describes oscillating flows, and used in this project to describe vortex formation and shedding behind the cylinder.

$$S_r = \frac{fL}{U_0} \quad (51)$$

Where,

f= Vortex Shedding Frequency

L = Characteristic Length

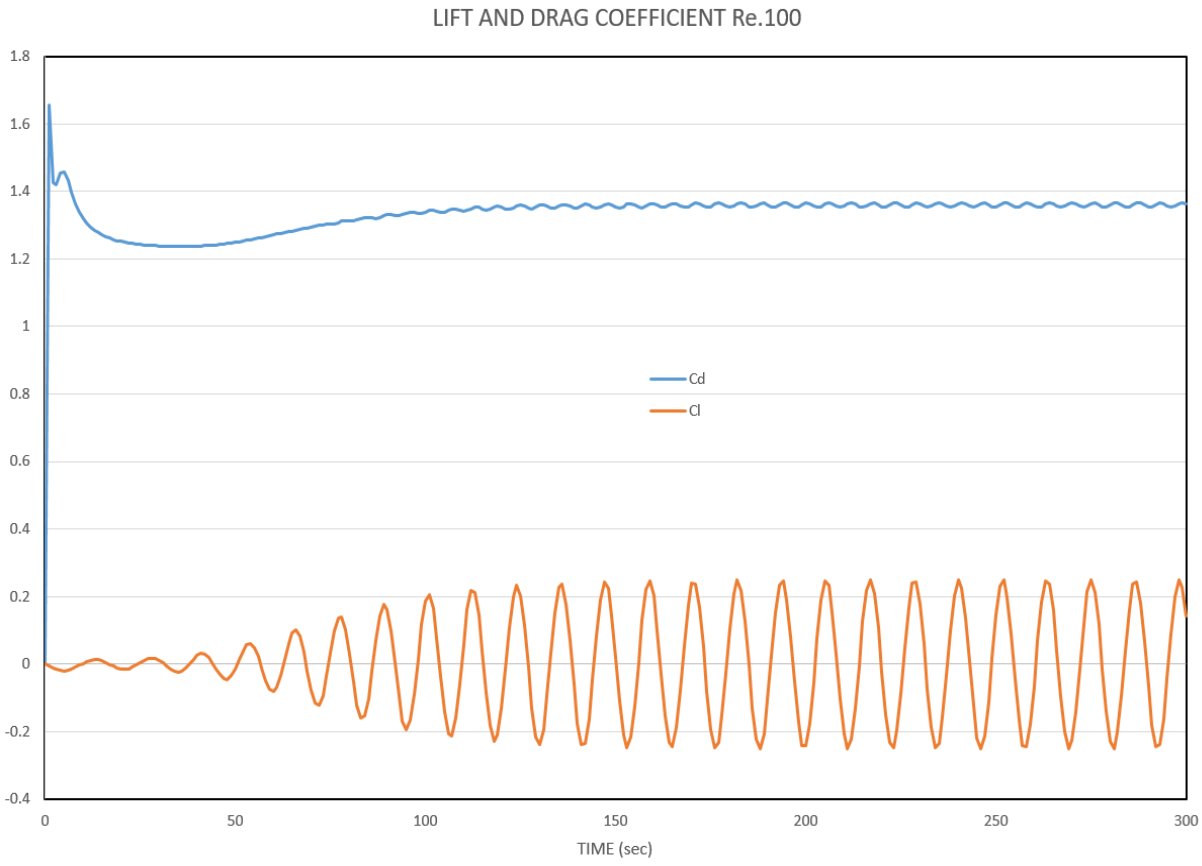

Figure 17: 2D Cylinder Lift and Drag Coefficient plot Re=100

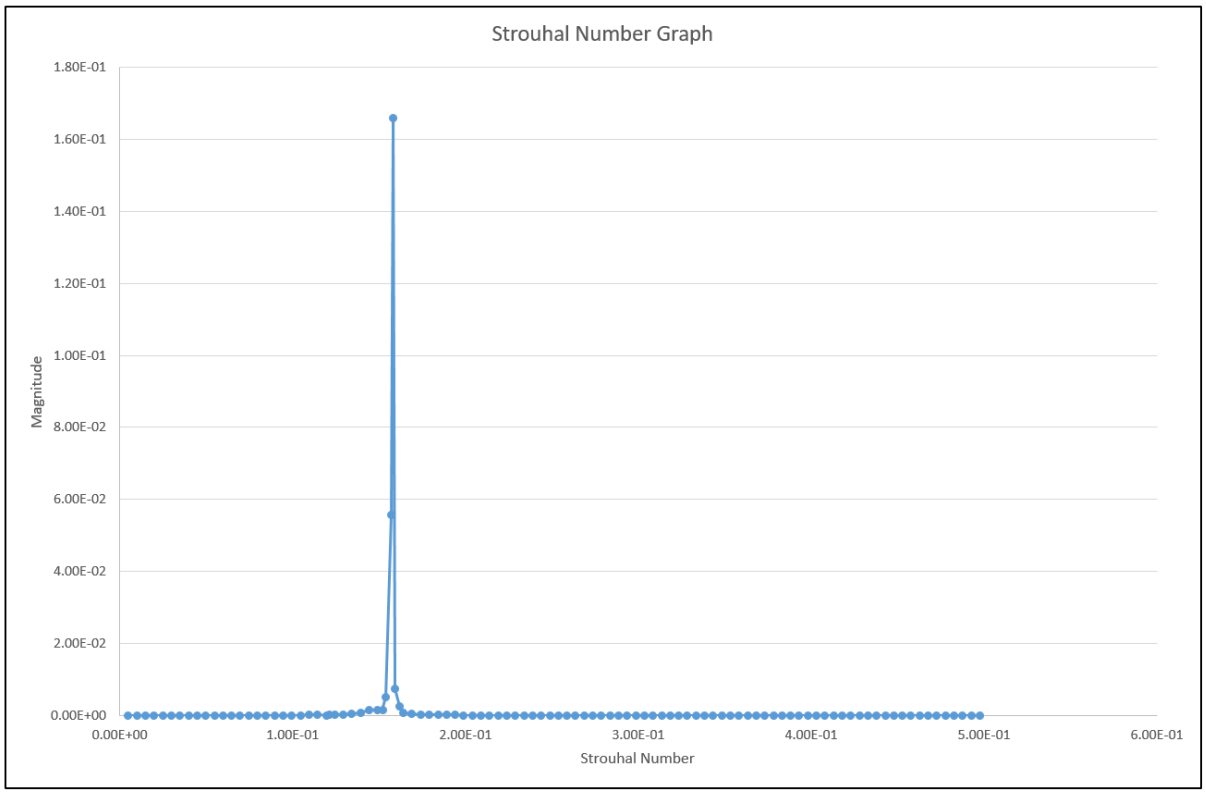

Figure 18: 2D Cylinder Strouhal Number Re=100

Table III: Comparison of Results for 2D Flow around a Circular Cylinder at Re 100

2D Flow around a Circular Cylinder @ Re=100			
	Graham [5]	Dr. Allievi and Dr. Bermejo [1]	This Project
Strouhal Number	0.16	0.167	0.158
Mean Drag Coefficient	1.25-1.46	1.295	1.33
RMS Value of fluctuating Drag Coefficient	0.042-0.04	0.0085	0.0062
RMS Value of fluctuating Lift Coefficient	0.157-0.39	0.162	0.170

- Conclusion

From the above flow visualization, we see that there is vortex formation when there is a flow past the circular cylinder, the vortex formation is initially symmetric till 10 sec, then its starts to lose its symmetry. After 30 sec, the streamline starts to oscillate forming von Karman vortices which becomes very visible at 40 sec. This vortex formation is due to the **suction effect** caused by the low pressure region behind the cylinder created by fast moving fluid past it. Combining the lift coefficient plot with flow visualization, we see that due to the symmetry in vortex formation during the first 20 sec of the flow, the lift coefficient is very close to zero (zero lift coefficient). When the Von Karman vortex starts to form after 30 sec, we see the lift curve start to oscillate with increase in amplitude which continues till 80sec. This section of fluid flow gives rise to Strouhals number of 0.158. We also note that in this region of low, the drag experience larger deviation than lift. The flow visualizations and with lift and drag coefficient graphs results, show a good agreement with the results published by Allievi and Bermejo [1] , and Graham [5].

4.3. 3D Flow Around Circular Cylinder For Re =100

4.3.1. Geometry Modelling

CATIA Part design is used to **create the 3D box using the pad function** and CATIA **pocket function is used to make a through hole** equal to that of the cylinder is made. The resulting CATIA file is saved as an IGS file to be imported to ANSYS Fluent for meshing.

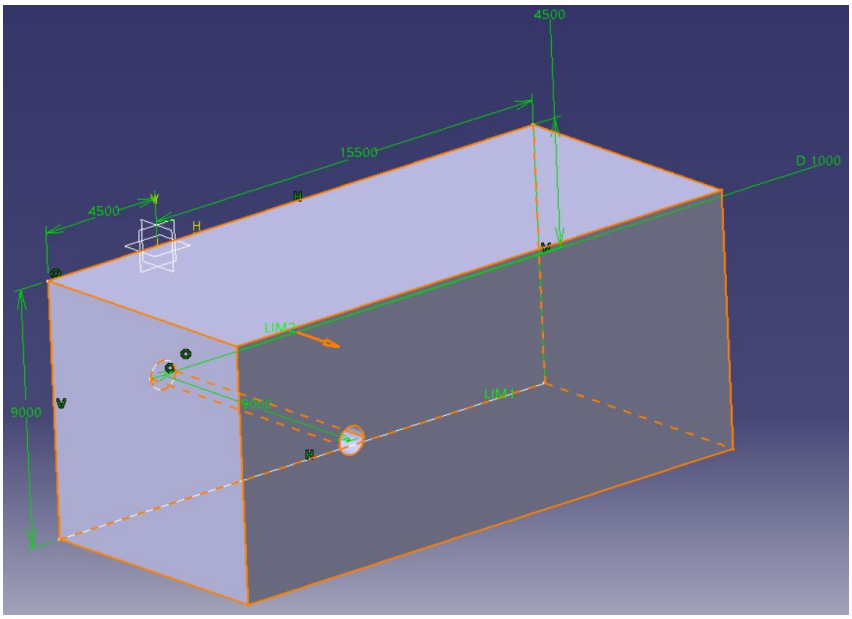

Figure 19: Final CATIA Outcome of 3D Cylinder in a Tunnel

4.3.2. Geometry Meshing

For this flow problem mesh, another complex approach is used. A fine mesh with relevance centre set to 100 (this ensures a very small element size). Inflation is applied to the cylinder boundary to create a boundary layer mesh as shown below.

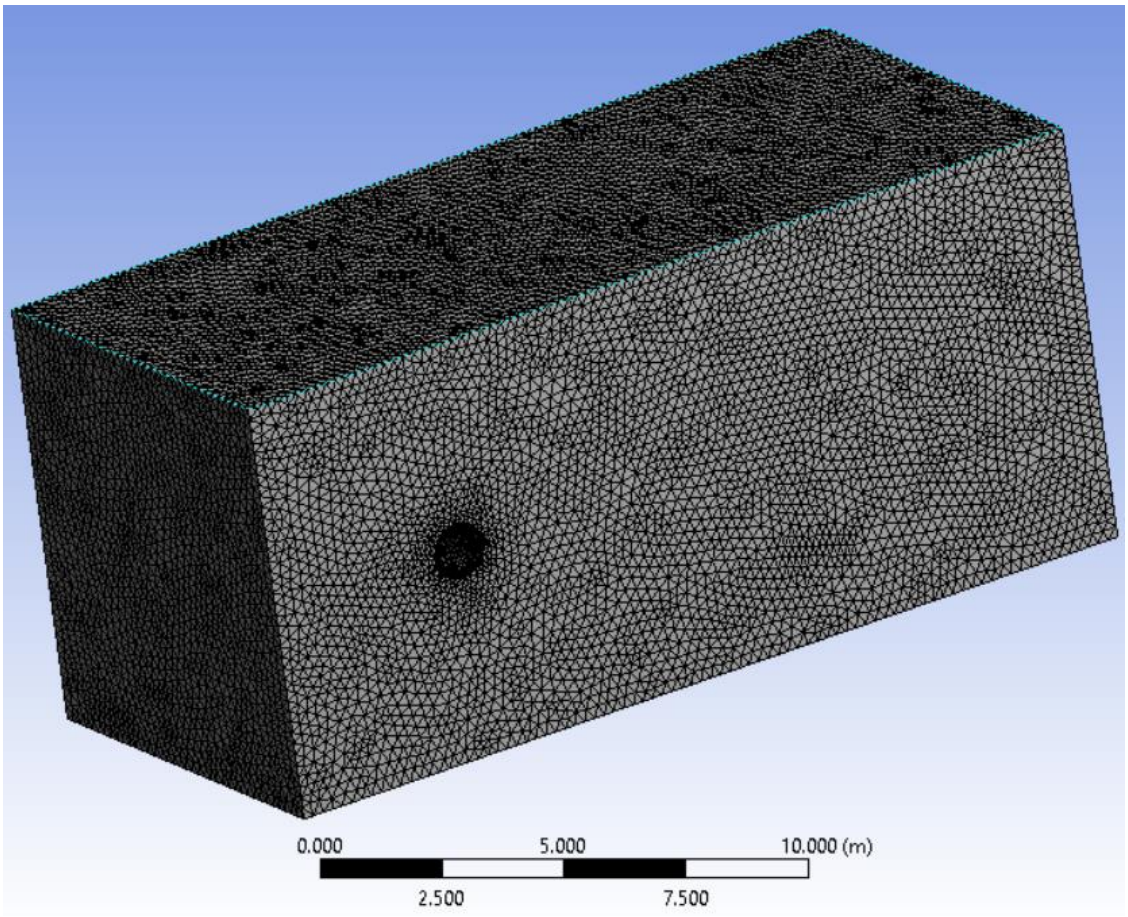

Figure 20: 3D Flow over a Cylinder Final Mesh Outcome

4.3.3. Computational Conditions

Table IV: Computational Condition for 3D Flow around a Circular Cylinder at Re 100

Problem No	Reynolds No	Mesh Divisions	Nodes
1	100	Relevance centre set to 100 and inflation at the boundary. Max face size = 0.23m (for non-bound layer mesh)	132168

4.3.4. Flow Conditions

For this flow problem Re is kept at 100 and,

$$\boldsymbol{Re} = \frac{\rho \boldsymbol{UD}}{\mu} \quad \textbf{(52)}$$

$D = Characteristic\ Diameter = 1m$

Assume Velocity U = 1m/s then,

$$\mu = \frac{\rho \boldsymbol{UD}}{\boldsymbol{Re}} \quad \textbf{(53)}$$

$$\mu = \frac{\mathbf{1 * 1 * 1}}{\mathbf{100}} = \mathbf{0.01 Ns/m^2}$$

NOTE:

- **Viscous Laminar pressure based solver** model is used for solving the above flow
- Flow velocity = 1m/s
- Time stepping method = Fixed
- Time Step Size = 1 sec
- Total number of time Steps =300
- Total Time (Total number of time Steps * Time Step Size) = 300sec
- Max number of Iterations per time step = 20
- Data recording time interval = 10 sec

4.3.5. ANSYS Modelling Output

➢ 2D Flow around a Circular Cylinder @ Re=100 Streamline Visualization

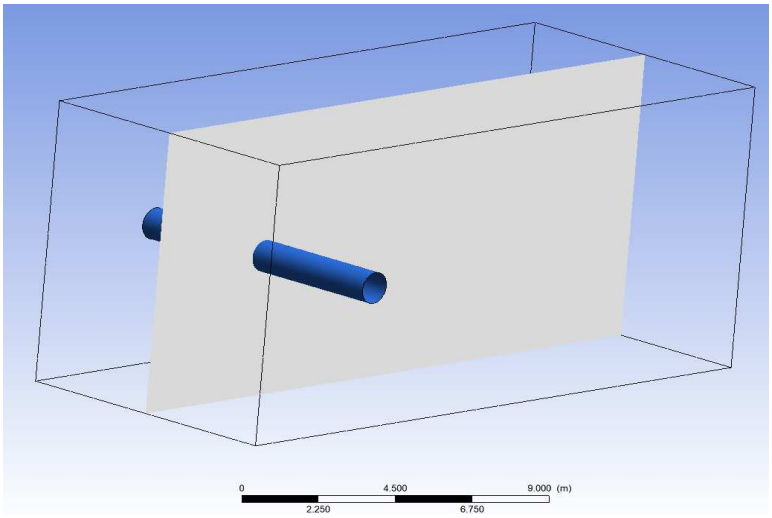

Note: The results are presented in 2d plane for better visualization

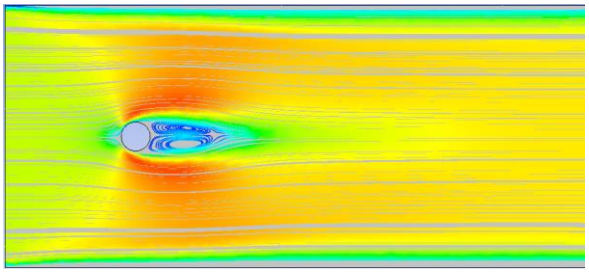

Time =10

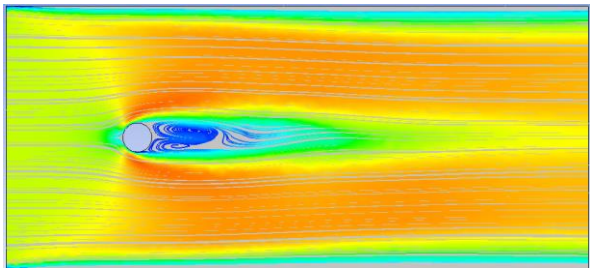

Time =20

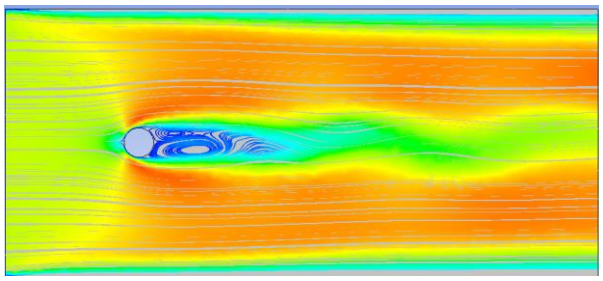

Time =30

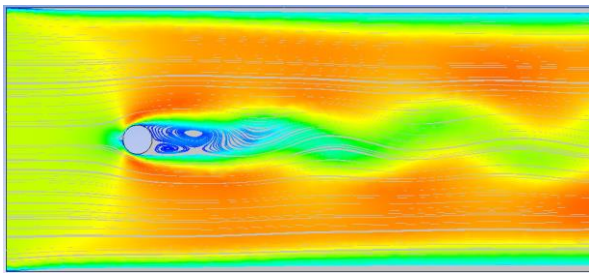

Time =40

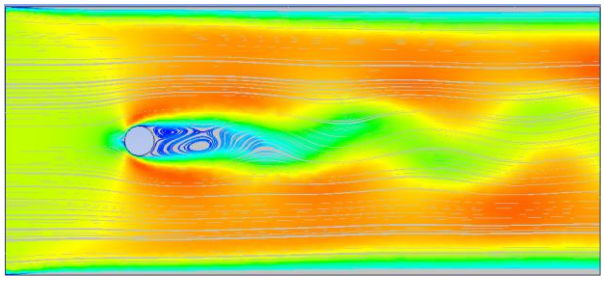

Time =50

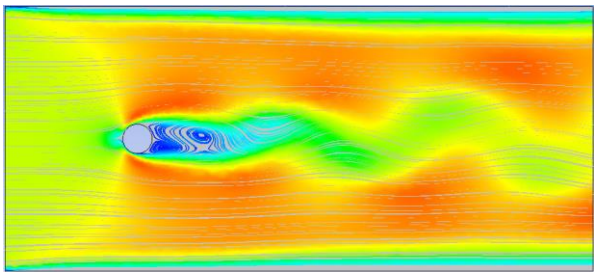

Time =60

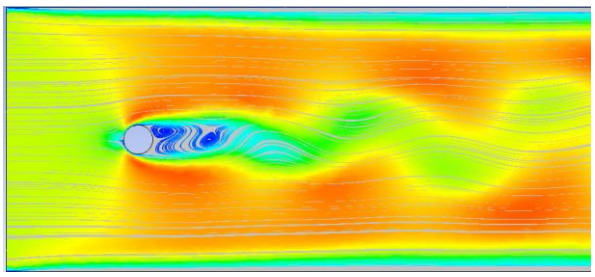

Time =70

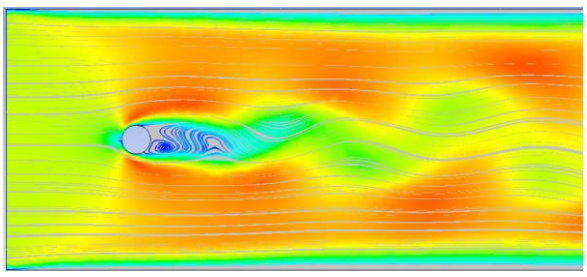

Time =80

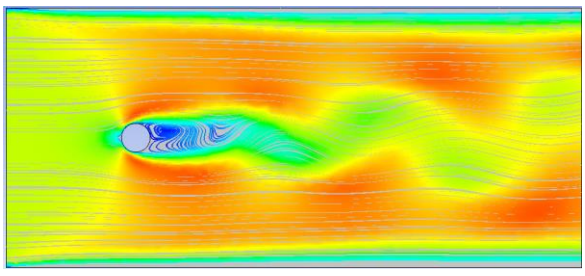

Time =90

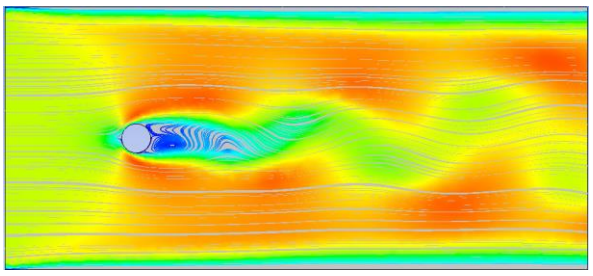

Time =100

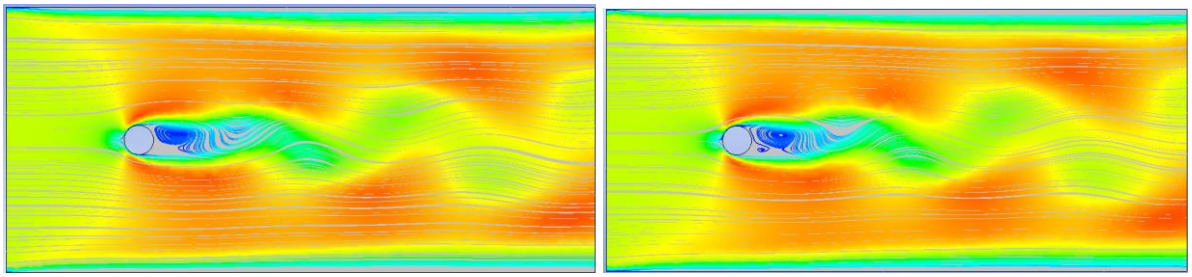

Time =110 Time =120

Figure 21: 3D Flow around a Circular Cylinder @ Re=100 Streamline Visualization

4.3.6. Conclusion With Lift and Drag Coefficient plot

- Drag Co-efficient (C_d)

Drag co-efficient is a non-dimensional number which represents the combined effect of friction drag and the pressure drag is derived by dividing drag force with dynamic pressure.

$$C_{d(Total)} = C_{d(Friction)} + C_{d(Pressure)} \quad (54)$$

$$C_{d(Total)} = \frac{F_d(Friction)}{\frac{1}{2}\rho U_0^2 S} + \frac{F_d(Pressure)}{\frac{1}{2}\rho U_0^2 S} \quad (55)$$

Where,

F_d = Drag Force

U_0= Free Stream Velocity

S= Surface Area

- Lift co-efficient (C_L)

Lift co-efficient is also, the ratio of lift force to the dynamic pressure.

$$C_{L(Total)} = C_{L(Friction)} + C_{L(Pressure)} \quad (56)$$

$$C_L = \frac{F_L(Friction)}{\frac{1}{2}\rho U_0^2 S} + \frac{F_L(Pressure)}{\frac{1}{2}\rho U_0^2 S} \quad (57)$$

Where,

F_L= Lift Force

- Strouhal Number (Sr)

Is a dimensionless number that describes oscillating and used in this project to describe vortex formation and shedding behind the cylinder.

$$S_r = \frac{fL}{U_0} \quad (58)$$

Where,

f = Vortex Shedding Frequency

L = Characteristic Length

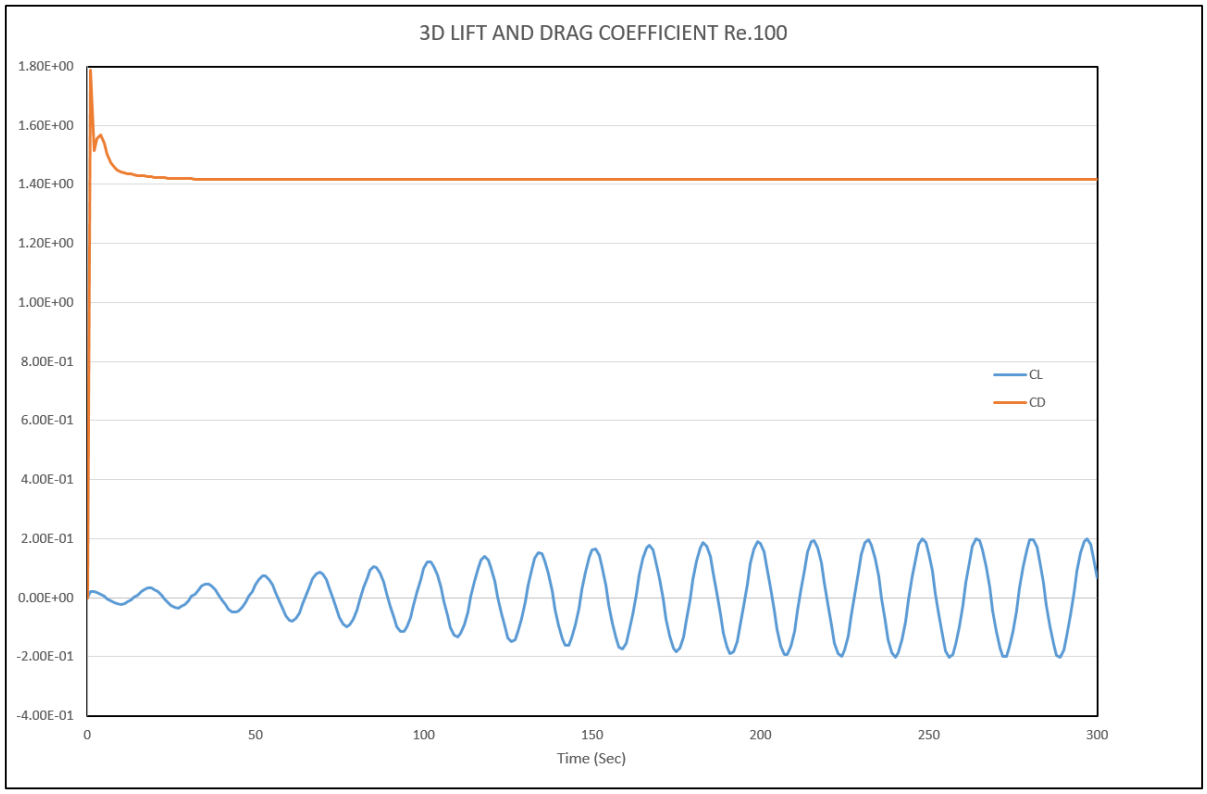

Figure 22: 3D Cylinder Lift and Drag Coefficient plot Re=100

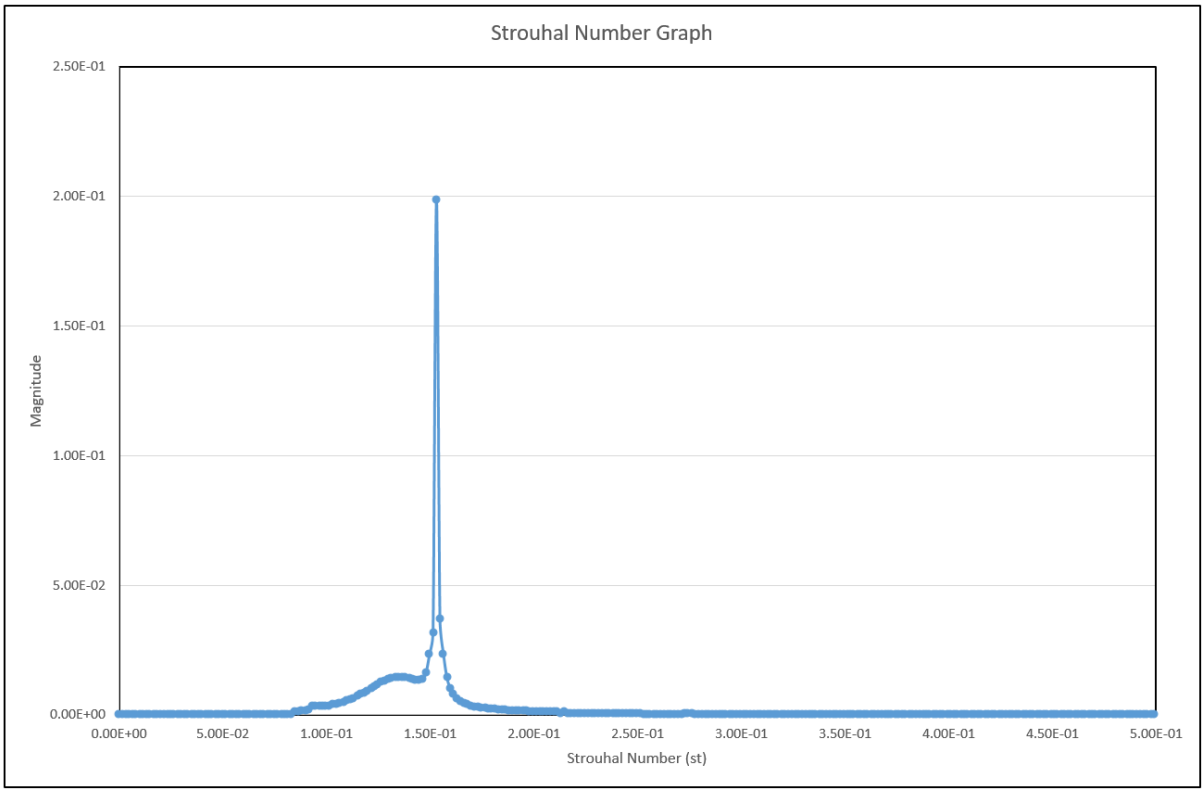

Figure 23: 3D Cylinder Strouhal Number Re=100

Table V: Comparison of 3D Flow Results

3D Flow around a Circular Cylinder @ Re=100			
	Graham [5]	Dr. Allievi and Dr. Bermejo [1]	This Project
Strouhal Number	0.16	0.167	0.153
Mean Drag Coefficient	1.25-1.46	1.295	1.42
RMS Value of fluctuating Drag Coefficient	0.042-0.04	0.0085	0.001
RMS Value of fluctuating Lift Coefficient	0.157-0.39	0.162	0.146

➢ Conclusion

From the above flow visualization, we see that the vortex formation and oscillation (Von-Karman vortices) is a bit similar to that of 2D but with some key difference.

Difference between 2D and 3D flow around a circular cylinder.

From the above graphs we observed

i. The 3D Mean drag coefficient is **greater than 2D** (1.42 > 1.33)
ii. The 3D RMS value of fluctuating Lift coefficient is **Less than 2D** (0.146 < 0.170)
iii. The RMS value of fluctuating Drag coefficient is zero (there is negligible oscillation in drag)
iv. Strouhal number for 3D and 2D are 0.153 and 0.153 respectively
v. In 2D, Cl fluctuation amplitude becomes steady at 130sec while in 3D the Cl amplitude becomes steady at 180sec

From the above, we draw conclusion that the differences between 2D and 3D flow around a circular cylinder, are caused by the additional viscous interaction between the cylinder and the sidewalls in 3D flow.

In all, the flow visualizations and with lift and drag coefficient graphs results, show a good agreement with the results published by Allievi and Bermejo [1] , and Graham [5].

5. OVERALL CONCLUSION

ANSYS Fluent is used model and the effects of viscosity in 2D lid driven cavity flow (at Reynolds numbers 3200 and 10000) and 2D and 3D flow around a circular cylinder. ANSYS fluent pressure based numerical algorithm is used for computation and the results obtained from the flow problems are compared to **analytical results** obtained by researchers like Dr. Allievi and Bermejo (viscous flow modelling using Finite element modified method of characteristics for Navier–Stokes equations) [1] and U. Ghia, K. Ghia and C. Shin (viscous flow modelling of High-Re problems using the Navier–Stokes equations and a multigrid method) [2] and, also **experimental results** obtained by researchers like Graham (The effects of waves on vortex shedding from cylinders) [4] and Koseff and Street (The lid-driven cavity flow: a synthesis of qualitative and quantitative observations) [5]. While using ANSYS fluent ready made algorithim for our viscous flow modelling, we created our own boundlayer meshes and calculation time steps to ensure very accurate results. Results obtained from our 2D lid driven cavity flow (flow visualization and velocity components plots along mid planes) shows strong aggrements with analytical and experiemntal data published and also, our 2D and 3D flow around a cylinder results (like lift and drag coefficent plot, Strouhals number and flow visualizations) are in lock step with experimental and analytical data available. Therefore the use of ANSYS fluent in visous flow modeling was carried out successfully.

6. REFERENCES

[1] A. Alejandro and B. Rodolfo, "Finite element modified method of characteristics for Navier–Stokes equations.," *International Journal for Numerical Methods in Fluids. 32. 439-463. 10.1002/(SICI)1097-0363(20000229)32:4<439::AID-FLD946>3.0.CO;,* vol. 32, no. 4, pp. 439-463, 2000.

[2] U. Ghia, K. Ghia and C. Shin, "High-Re solutions for the incompressible flow using the Navier–Stokes equations and a multigrid method," vol. 48, p. 387, 1982.

[3] J. Koseff and R.L.Street, "Visualization studies of a shear driven three-dimensional recirculation flow," *ASME,* vol. 106, p. 21, 1984.

[4] J. K. a. R.L.Street, "The lid-driven cavity flow: a synthesis of qualitative and quantitative observations," *ASME,* vol. 106, p. 390, 1984.

[5] J. Graham, "The effects of waves on vortex shedding from cylinders," in *IUTAM Symposium on Bluff-Body Wakes Dynamics and Instabilities*, Gottingen, Germany, 1992.

[6] J. Benque, B. Iblier, G. Labadie and A. Keramsi, "A finite element method for Navier–Stokes equations coupled with a temperature equation," in *Fourth International Symposium on Finite Elements in Flow Problems*, North-Holland, Amsterdam, pp 295-301., 1982.

[7] O. Pironneau, "On the transport-diffusion algorithm and its applications to the Navier–Stokes equations," *Numer Maths,* vol. 38, pp. 309-322, 1982.

[8] P. Deak, "Peter's Engineering," 22 June 2015. [Online]. Available: http://petersengineering.blogspot.com/2015/06/navier-stokes-equation-for-3d.html. [Accessed 1 June 2019].

[9] Glenn Research Center, NASA, 05 May 2015. [Online]. Available: https://www.grc.nasa.gov/www/k-12/airplane/nseqs.html. [Accessed 01 June 2019].

[10] ANSYS Inc, "ANSYS Fluent Theory Guide.," ANSYS Inc, 2010.

[11] J. Douglas and T. Russell, "Numerical methods for convection-dominated diffusion problems based on combining the method of characteristics with finite difference procedures," *SIAM J. Numer Anal,* vol. 19, pp. 871-885, 1982.